

Investigating shear behaviour of fibreglass rock bolts reinforcing infilled discontinuities for various pretension loads

Peter Gregor¹, Ali Mirzaghobanali¹, Kevin McDougall¹, Naj Aziz^{1,2}, Behshad Jodeiri Shokri^{*1}

1.School of Engineering, University of Southern Queensland, Springfield Campus, Springfield, Australia

2.School of Civil, Mining, and Environmental Engineering, University of Wollongong, NSW, 2500, Australia

* Corresponding author. School of Engineering, University of Southern Queensland, Springfield Campus, Springfield, Australia; Tel:+61416080049; E-mail address: Behshad.JodeiriShokri@usq.edu.au

Abstract

In this paper, eight shear tests were carried out utilising a double shear with infilled shear interfaces after determining an appropriate experimental design and modified testing scheme. For this, two rock bolts, 20-tonne and 30-tonne, were tested with modified double shear testing apparatus at different pretension loads. The infilled test scheme was conducted with 5mm thick sandy clay infilled shear interfaces. A 40MPa small aggregate concrete was used for all samples to simulate the host rock. Based on the shear profiles, it was found that all samples followed a three-part failure profile consisting of elastic, strain softening and failure regions. The results of double shear tests revealed that the 20-tonne rock bolt saw a significant overall decrease of approximately 30% in its failure displacement response as opposed to the 30-tonne samples' which saw a 6% increase. Also, it was concluded that the 30-tonne samples outperformed the 20-tonne rock bolts by up to 30%, irrespective of initial pretension settings. Comparing the physical failure characteristics of the samples found that both the 20-tonne and 30-tonne samples exhibited the same response to increased pretension. As the pretension increased, the angle experienced at the hinge point also increased incrementally.

Keywords: Fibreglass; double shear test; infilled joints; pretension load

1. Introduction

Tendons are used as part of support systems to stabilise strata and are generally divided into two main categories: cable bolts and rock bolts. While both rock and cable bolts provide strata reinforcement, their design implementations are different. Rock bolts are mostly installed as part of the active reinforcement system while cable bolts are installed for either pre or post reinforcement (Windsor, 1997). Rock bolt systems were first introduced for use as mining ground supports during the late 1940s (Mark, 2017). Within a year of inception, rock-bolts tested in soft rock systems proved to be highly successful by improving safety for heading works and allowing for better utilisation of excavated areas (Conway, 1948). Since then, applying rock bolts' reinforcement has been adopted by industry for several decades. They have become popular and cost-effective products for ground control by ensuring system safety and design longevity in both mining and civil applications.

Projects implementing rock bolt strata support systems need to evaluate each property of rock bolts to determine suitability and optimum performance. Due to environmental and operational constraints of metal rock bolts, alternatives such as fibreglass rock bolts can provide unique benefits to the system, but their capabilities need to be further explored. Unlike steel, fibreglass rock bolts are a combination of two primary elements; linearly aligned glass fibres and thermo-set resin (Frketic et al. 2017). As such, the resultant rock bolt is comprised of a uniaxial structure that results in anisotropic performance (Maranan et al. 2015) in stark contrast to the isotropic matrix of

metallic rock bolts. The effects of the differing structures are observed in the following key areas: load transfer mechanisms, lightweight, application limitations (i.e., corrosive environments), and cutability. The study conducted by Aziz et al. (2015b) investigated the difference of isotropic and anisotropic rock bolts and concluded that axially loaded fibreglass rock bolts can achieve up to 85% of the ultimate tensile strength of steel. However, when loading the sample perpendicular to the fibre direction (i.e., shear loading) the rock bolt's shear failure load averaged only 25% of the metallic rock bolt. The low shear performance of fibreglass rock bolts has limited their use to rib reinforcements where limited shearing is present (Li et al. 2016). Despite reduced performance limits to that of metallic rock bolts, fibreglass rock bolts possess significant benefits to their metal counterparts: including cutability and corrosion resistance. During coal extraction, rib supports are often removed with the advancement of shearers. Fibreglass rock bolts are often chosen over metallic rock bolts as the shearer heads can safely cut the fibreglass rock bolts without inflicting damage during the extraction (Gilbert et al. 2015). Additionally, studies conducted by Hassell et al. (2004), Spearing et al. (2010) and Aziz et al. (2013a) outlined the detrimental effects of corrosion on metallic rock bolts and their susceptibility to such environments. Aziz et al. (2013b) outlined the four key forms of corrosion impacting steel as uniform, localised, mechanically assisted degradation and environmentally assisted degradation. Due to the non-metallic nature of fibreglass rock bolts, they demonstrate an improved level of resistance to corrosive environments. As a result, fibreglass rock bolts are commonly implemented as supports in highly corrosive environments such as coal mines.

All rock bolt types are subject to two main loading behaviours along their length: axial, and shear loading (Chang et al. 2017; Clifford et al. 2001; Forbes et al. 2020; Hartman, 2003; Jahangir et al. 2021; Jodeiri Shokri et al. 2023; Rajapakse, 2016; Li et al. 2017b; Mirzaghobanali et al. 2017; Nourizadeh et al. 2023; Thenevin et al. 2017; Thompson et al. 2014; Waclawik et al. 2019; Windsor et al. 1992). Axial loads are the stresses acting along the longitudinal length of the bolt. As such, the primary component of axial forces is determined by vertical stresses (Nemcik et al. 2006). While the load transfer mechanisms are the bolt's response to axial loading, it is complicated and dependent on several factors. As a result, many research and experimental works such as tensile load testing (VandeKraats et al. 1996), push testing (Aziz et al. 2016), and pull-out testing (Mirzaghobanali et al. 2017) have been conducted for understanding the load transfer mechanism for several decades.

Due to the differing tectonic forces translated across varying strata, significant shearing forces are exerted along the bedding planes and onto rock bolts (Nemcik et al. 2006). Indeed, the intensity of the shearing forces is dependent on the stiffness of the bedding plane. It means that the observed shear loads induce resistive forces along the shear displacement plane and opposite to that of the applied load. Unlike axial load transfer tests, shear

load transfers are limited to laboratory testing. Due to the difficulties of determining the localised shearing forces located within in situ strata, numerous studies have been conducted to determine the shearing properties of the rock bolts and cable bolts (Li et al. 2016, Song et al. 2008, Aziz et al. 2015a). The shearing performances of rock bolts can be determined using several methods each with a varying representation of the bolts in situ conditions. Shearing tests developed include (1) the single shear guillotine test in accordance with the British Standard for testing (2009), (2) the double shear guillotine test, and (3) concrete embedded double shear testing (Gilbert et al. 2015). It should be noted testing requirements for rock bolts and cable bolts are identical and various adaptations to these test methods have been developed (Li et al. 2017b).

Single shear testing is accomplished by cutting the tendon along a single plane. According to Li et al. (2017b), single shear testing does not accurately determine shear strength properties as the: (a) rock bolt is not encapsulated inside concrete medium, thus not representing rock strata; (b) single shear testing overestimates the shear strength of the cable bolt due to the two opposing metal frame bodies contacting during shearing (Aziz et al. 2015a), and (c) single shear testing is a passive shear test whereby the rock bolt is sheared without pre-tensioning. It is noteworthy that three testing systems for single shear testing including the British Standard (2009) single shear test (BSST), direct single shear and the Megabolt single shear tests have since been developed and are still in use today (Aziz et al. 2017). Each test evaluates different aspects of the tendon's performance.

Due to the presence of strata bedding, multiple shear planes can be induced on a single bolting system (Nemcik et al. 2006). As a result, the double shear testing method was developed to simulate the actual field conditions. The double shear testing apparatus consists of a single bolt grouted into three concrete blocks as first developed by Aziz et al. (2003). Double shear testing methodology was designed with three types namely MKI, MKII and MKIII (Aziz et al. 2016). MKIII is the modified version of MKII and both are used for the shear strength determination of high strength tendons such as cable bolts. The double shear box is comparable to Megabolt shear test as it incorporated simulated concrete strata to replicate the effects of localised crushing (Aziz et al. 2015a). The double shear box was initially used for the investigation of varying host strata UCS. The study conducted by Gilbert et al. (2015) using the MK1 double shear apparatus provided an understanding of the relationship between shear strength and host UCS by subjecting rock bolts to host rock strengths of 40MPa and 60MPa. As a result, the study observed two unique and increasing ultimate shear failure loads and concluded that the shear performance of rock bolts was a function of the host rock UCS. Gilbert et al. (2015) used the MK1 double shear testing apparatus from the Aziz et al. (2003) study to also compare the shear load transfer mechanisms of fibreglass rock bolts using the single shear testing method (i.e., Guillotine box). A limited number of tests were carried out on

fibreglass rock bolts using double shear testing method (MKI). When compared to the single shear test method, it was concluded that (a) single shear testing of guillotine box underestimates the shear strength of fibreglass rock bolts; (b) shear strength of fibreglass rock bolts is a function of pretension values, and (c) strata strength (i.e., concrete strength) affects the shear strength of fibreglass rock bolts. Furthermore, Li et al. (2016) identified the mechanism whereby the weaker host rock crumbles at the shearing plane allowing the rock bolt to flex inducing additional stresses on the rock bolt element. Samples tested at 60MPa were identified as less susceptible to this phenomenon and as such indicated that an increase in the host rock UCS resulted in an increase in the overall shear performance of the rock bolts. The MKI double shear box was further modified to allow for the investigation of varying bolt pretensions. The study conducted by Aziz et al. (2015b) adopted the MKI double shearing apparatus to investigate the effect of pretension on the shear performance of rock bolts. Pretension values of 2.5, 5, 10 and 15kN were chosen for the study and despite the non-uniform distribution of pretension values the study highlighted an increase in the ultimate shear failure in the presence of pretension. MKI is the suggested testing method for non-metallic rock bolts such as fibreglass bolts as per Aziz et al. (2015b).

Contrary to the discussed studies, there is significant variation in real-world scenarios between the surfaces of the shearing planes, including friction and infill material. As a result, both clean and infilled joints are susceptible to asperity properties that impact their overall shear performance. Barton (1971) statistically analysed the joint properties of varying roughness by mapping the asperities from re-created shear tests with high normal stresses. One of this study's outcomes was categorising the asperity profile, which later developed into the roughness profile classification. This classification is still in use with studies adopting the profiles to test the shear behaviour of infilled joints with 3D printed studies conducted by Mirzaghobanali et al. (2022). While Barton (1971) focused on clean joints, it also developed the foundation for analysing the shear strength of filled joints, as later explored by Barton (1973), where the shear characteristics of four examples of infilled joints were defined.

The literature review revealed that, few of the identified research investigated fully grouted fibreglass rock bolts of various tensile ratings, installed with various pretension settings, subjected to shearing. There were also limited studies investigating the impact of infilled shear interface on various tensile rated fibreglass rock bolts' shear performance. Therefore, the main objectives of this research are (a) determining an appropriate experimental design and testing scheme to suitably test the shear performance of fibreglass rock bolts and (b) undertaking a comprehensive experimental study to determine the shear strength of two fibreglass bolts under varying pretension values for infilled joint interfaces. Indeed, this research will answer following questions: (a) how does the application of pretension affect the shear load transfer mechanism and final shear performance of fibreglass rock

bolts? (b) What are the impacts of infilled shear interfaces on the shear load transfer mechanisms and ultimate shear performance of fibreglass rock bolts?

2. Materials and Methods

2.1. Experimental Design

In general, the shearing performances of rock bolts can be determined using a number of methods each with varying representations of the bolts *in-situ* conditions. Shearing tests developed include the single shear guillotine test in accordance with the British Standard for testing (2009), the double shear guillotine test and concrete imbedded double shear testing (Gilbert et al. 2015). Testing requirements for rock bolts and cable bolts are identical with various adaptations of these tests developed (Li et al. 2017b). The shear behaviour of rock bolts can be determined using single and double shear testing. The British Standards single shear test scheme is achieved by grouting the rock bolt or cable bolt within a metal guillotine frame and according to Li et al. (2017b). This test scheme does not accurately determine shear strength properties due to the method of encapsulation, system design flaws and inability to test active systems.

The single shear test method was further developed by McKenzie et al. (2015) with the development of the Megabolt shear test apparatus. This test method required the bolt to be grouting into concrete. The Megabolt testing machine was exclusively designed for high strength cable bolts where the length of encapsulation could go up to 4 meters (Li et al. 2017b). Li et al. (2017b) also highlighted significant differences between the MSST and BSST testing methods and conversely strong correlations with the shear profile of the double shear testing apparatus. The double shear test apparatus developed by Aziz et al. (2003) and revised at the University of Wollongong (Li et al. 2016) provided a mode of testing that improved the accuracy of the shear failure mechanism of clean plane surfaces for rock bolts and cable bolts. However, there are still a number of short comings to the testing method including the lack of ability to determine the impacts of infilled discontinuities and the interference from the supporting frame. For this, in this research, it was extended to include the effects of the shear plane surface (i.e. infill joints) on the fibreglass bolt's performance. This was accomplished by bonding the sandy/clay infill material to the shearing plane. The joint infill study was conducted primarily with a homogeneous shear interface relationship to allow for cross validation with the initial clean interface double shear testing apparatus. It was essential to maintain a uniform testing procedure for infill joints due to the limited understanding of the latter.

2.2. Experimental plan for infilled discontinuities

Testing was conducted on several fibreglass rock bolts with commonly used load capacity ratings of 20 and 30-tonnes. The rock bolts had a nominal diameter of 18mm and were 1.2m in length with threads at both ends. Double shear testing was conducted through investigating the effect of bolt strength on the shear performance of fibreglass rock bolts at a range of pretension values. Fibreglass rock bolts of various strengths were tested to determine the rock bolts performance on a passive rock bolt system (i.e., no pretension). The results formed the baseline performance data of rock bolts for a simplified uniform environment. The strata UCS value was chosen following the study conducted by Li et al. (2016). This study identified the host strata UCSs of 20MPa, 40MPa and 60MPa as an accurate representation of field conditions. The 40 MPa concrete strength was then chosen for casting simplicity. Additionally, wet concrete at a target strength of 40MPa was found to have ideal workability. The weaker 20MPa and stronger 60MPa mixtures were either too wet or too stiff to handle efficiently. The second experimental study explored the effects of varying pretension values on the shear strength of fibreglass rock bolts. To maximise sample uniformity, a single host media strength of 40MPa was used. The fibreglass bolts were fastened using their respective nuts and washers and torqued to pretension values of 0%, 5%, 10% and 15% of the maximum tensile load capacity of each rock bolt in accordance with industry standards as indicated by Gilbert et al. (2015). The prepared samples were then sheared at the rate of 1 mm/min (Gilbert et al. 2015). It is noteworthy that, the infill joint experimental study was divided into two following investigations, namely:

- (a) The effects of a sandy clay infill joint on the shear performance of fibreglass rock bolts.
- (b) the impact of a range of pretension values on the shear performance of fibreglass rock bolts subjected to infilled conditions.

The double shear testing method was extended to infilled joints whereby joints were separated by 5 mm of the infill material at initial moisture content of 20%. The type, thickness, and moisture content of infill material were selected based on studies by Oliveira et al. (2010) and Mirzaghorbanali et al. (2014). To ensure consistent interface performance and sample preparation consistency, the infill materials were sourced from one batch to prevent the impact of product quality variations. The infill was then prepared in a large batch to apply to the entire test scheme to minimise mixture variance. As outlined in Table 1 eight tests were conducted to test two FRP rock bolts under varying pretensions.

Table1: Experimental plan for reinforced concrete blocks with infilled joints

2.3. Equipment design

Double shear testing was carried out using the 150 tonne compression testing machine at the Engineering laboratory of the University of Southern Queensland. The prepared samples were positioned inside of the testing

machine and then subjected to shearing at the shearing rate of 1 mm/min (Gilbert et al. 2015). The shear displacement was exerted on top of the middle block by a levelling load plate and the shear load measured using a calibrated load cell as highlighted in Figure 1. The load cell was attached directly to the shearing plate and the data collected using an inbuilt data acquisition system.

Figure 1: Outline of SANS Machine used for double shear testing

2.4. Shear box

In order to provide confinement around the concrete block during shear testing, a steel shear box shown in Figure 2 was designed and manufactured according to the samples' dimensions and as per the shear testing procedure (Li et al. 2016). The confinement impeded premature failure of the concrete blocks during shear testing, allowing fibreglass to achieve its maximum shear strength capabilities. In civil and mining field conditions, confinement is provided naturally via surrounding strata.

Figure 2: MK1.5 Double shear box design

The overall length of the confining box was 780mm with the total concrete length being 800mm. The 20mm difference in length created a 10mm allowance for the shearing plans. It was essential to minimise the unencapsulated surface area and maintain symmetry as the exposed area encounters different confinement pressures and has the potential to cause premature concrete failure around the jointed section. As such, the 20mm spacing was applied 5mm to each side of the shearing plane as illustrated in Figure 3.

Figure 3: Assemble double shear apparatus highlighting key features such 10mm spacing at each interface

The 5mm spacing on each side of the shearing plan successfully addressed the issues relating to frame wedging by the British standards testing method as depicted in Figure 1. Despite the British standard of testing measuring single shear performance, the rotation encountered during testing was also present during double shear testing as shown in Figure 4. It is noted that the addition of the 5mm spacer was successful with no evidence of frame wedging. While this method doesn't remove the presence of shear rotation it does successful minimise the potential of mechanical interference of the test frame at the shear planes.

Figure 4: Centre block rotation because of testing

2.5. Mould design

Moulds were constructed utilising the UniSQ workshop CNC facilities to ensure uniform casting parameters. Each mould was designed to produce three individual concrete blocks that were later assembled to form a system with two shear planes. The blocks of the outer edge of the double shear system were cast to the dimensions of 200mm

by 200mm by 200mm and the centre block to the dimensions of 200mm by 200mm by 400mm with a longitudinally intersecting hole with a radius of 16mm (Fig 5).

The mould consisted of a series of timber panels, metal dividers, braces and an intersecting PVC pipe. The braces were used to minimise mould deformation under the weight of the concrete during curing. To create a cavity for the rock bolt and to simulate the rifling that results from the drilling process, a rope was wrapped around the PVC pipe. Care was taken to not wrap the rope too tightly as initial attempts resulted in the rope exerting inward axial forces on the pipe increasing the difficulty of disassembly. Once the concrete was poured and levelled, PVC conduits were then inserted into the centre of each block intersecting the PVC pipe. The conduits create a small channel directly to the rock bolt location allowing for a simpler grout charging process. Excess concrete was then poured into 100mm diameter by 200mm steel moulds for future UCS testing.

Figure 5: Double shear mould design

2.6. Sample preparation

As per the experimental plan, the concrete blocks were cast to 40MPa specifications using a mortar recipe following the guidelines from Gilbert et al. (2015). Two specifications of concrete were cast with the first designed to achieve a UCS of 20 MPa and the second achieving 40 MPa. Initially the low strength 20MPa sample was cast using the cement, sand, and water ratio of 1:3:0.7, successfully resulting in a consistency like that of sandstone. Coarse sand was used instead of aggregate to maintain cross-sectional uniformity. By adopting a low strength mortar-based recipe, the initial testing of samples proved the mixture did not have sufficient strength to shear the rock bolt. Figure 6 shows the severe damage sustained by the concrete blocks prior to achieving failure within the rock bolt element. As such the mixture was adjusted to achieve a minimum strength of 40MPa using a cement, sand, and water ratio of 1:2.2:0.42.

Figure 6: Severe damage resulting from a weak concrete matrix.

The concrete production was completed using the climate-controlled facilities and curing room at the University of Southern Queensland to maintain the consistency and high-test quality. Each batch of concrete was mixed using the onsite concrete mixer and set into the moulds using a vibrator and scraper to remove bubbles and impurities resulting in clean uniform samples as shown in Figure 7. The concrete was left to set for 24 hours, after which the moulds were disassembled, and the blocks placed into the curing room for a minimum of 28 days. The 28-day curing period was essential for ensuring the concrete was at peak design strength.

Samples were capped using plaster of Paris to minimise the impact of stress concentrations forming from surface imperfections because of casting. The fine composition of the plaster fills the surface irregularities and facilitates

optimum transfer of forces. Prior to testing of the double shear blocks, the cylinders of the corresponding batch were tested under compression conditions to determine the actual host UCS. The UCS results are presented in Table 2 and indicate an average of 48MPa. All samples tested met the minimum strength requirements and as a result all double shear tests were successfully performed to achieve rock bolt failure prior to host medium failure. In addition, the cylinders were subjected to Brazilian testing methods to determine the equivalent tensile strength of the sample. Table 3 indicates an average tensile strength of 4.7MPa.

Table 2: UCS test results of the concrete used for double shear casting

Table 3: Brazilian testing of concrete used for double shear casting

Figure 7: (a) Cast of double shear sample; (b) concrete samples for UCS testing

2.7. Pre-tensioning

Once the concrete samples were cured, the fibreglass bolts were positioned into the precast holes for final assembly. The rock bolt, concrete blocks, axial loadcell and the washer plates were assembled loosely and in the correct order for final tightening. The pretension was then applied to the desired value as per the experimental plan in Table 1. The pretension (kN) was determined using the hollow load cell installed previously for the monitoring of axial loads. The pretension value varies between 0kN to 20kN similar to those currently applied in Civil and Coal Mining industries (Gilbert et al. 2015). The minimum pretension value of 0kN was achieved by installing wedges in the edge of the holes to overcome the weight forces of the washers, rock bolt and load cells and ensure the system was centred. The remaining pretensioned samples had sufficient axial loads to ensure the system was centred. In order to minimise the effects of creep and settling, all samples had their respective pretensions applied 24 hours prior to grouting.

2.8. Grouting

In the last stage of sample preparation, the reinforced concrete blocks were grouted through holes on top of the sample as shown in Figure 7a. Additional cube samples were cast as suggested by (Aziz et al. 2014) for measuring of the grout mechanical properties. As determined during preliminary testing, grout mechanical properties such as UCS, shear strength and elastic modulus are a function of time (Mirzaghornanali et al. 2018). The grouted sample was left undisturbed for a period of seven days prior to the shear box assembly. This ensured that the grout UCS was greater than that of the concrete blocks and that the initial curing stage of the grout was complete, to achieve consistent performance during shear testing.

Once the samples were cast and grouted, any excess grout was removed from the injection holes and then cleaned smooth to prevent stress concentrations. The sheared samples were then dismantled to investigate the grout

encapsulation quality. As demonstrated in Figure 8, the rock-bolt appropriately centred within the bore and the grout successfully encapsulated the entirety of the bolt with minimal voids. The highlighted section of Figure 8 illustrates the micro ridges formed by the rope technique adopted in section (2.4). The adopted techniques allowed for uniform encapsulation throughout the whole annulus area on all samples. Samples were left for an additional seven days to allow the grout/fibreglass interface to strengthen and ensure the grout strength exceeded that of the concrete.

Figure 8: Grouting quality examination after testing

2.9. Infilled discontinuities

Infilled material was applied to the double shear samples to assess the performance of rock bolts under more in-situ like shearing environments. An infill material comprised of sand and clay was created using a sand, clay and water ratio of 1:1:0.48 forming an easy-to-handle paste. This material was chosen as it replicates the composition of possible joint fill found in field environments (Mirzaghobanali et al. 2014). The manufacturing of the infilled samples remained largely similar to that of the clean joint preparation. To adapt the sample preparation to include infill materials the following steps were included to the clean sample preparation method. Prior to aligning the blocks in preparation for inserting the rock bolt, the infill paste was applied to the surface of the shear face of two outer blocks to a depth of 5mm using a scraper ensuring a hole was left for the dowel as shown in Figure 9a. Once both outer blocks were completed, they were aligned and lightly pressed into shape against the centre block. Any gaps were then filled and smoothed off as shown in Figure 9b. Finally, the edges of the shear plane were surrounded in tape to minimise drying as shown in Figure 9c.

Figure 9: (a) Layer of infill material on shearing plane of concrete section;(b) Close up of the mating of the shearing planes with infill material;(c) Minimising infilled drying during preparation

2.10. Initial Testing

2.10.1. Unconfined Shear Samples

Two preliminary double shear tests were carried out on reinforced concrete blocks without confinement. The results of the test were undertaken to trial the success and efficiency of the preparation method adopted. Tests were performed on 20MPa and 40 MPa concrete blocks reinforced with 30t fibreglass rock bolts with no confining pressure as can be seen in Figure 10. Bolts were set to passive mode (i.e., no pretension) and sheared at 1 mm/min shearing rate.

Figure 10: Initial unconfined test 30-tonne

After one day of curing, the prepared sample was positioned in the compression-testing machine. The peak shear load values were 5.7 and 8.5 t for 20 and 40 MPa concrete blocks, respectively. Due to samples being tested in an unconfined environment, the rock bolts did not achieve failure and the test became an analysis of the systems bending performance. Samples were carefully dismantled after testing to investigate the quality of grouting and encapsulation as shown in Figure 11. High quality encapsulations were observed for both the fibreglass bolt and concrete medium.

Figure 11: High quality encapsulation (left) around fibre glass bolt (right) around the concrete medium

2.10.2. Confined shear samples

The main double shear tests were carried out on reinforced concrete blocks using the MK1.5 designed confinement shear box as shown before in Figure 3. Tests were performed on 20MPa concrete blocks reinforced with 30 t fibreglass bolts. The bolt was set with a pretension of 10kN and sheared at 1 mm/min shearing rate. The first test conducted using the pretension of 10kN. It is evident that there is a significant axial transfer of load resulting in the pretension doubling to 22kN. Additionally, confined samples have also achieved a greater shear load to that of the preliminary study.

2.10.3. Infill material properties

Analysis on the infill soil properties were conducted to ensure a comprehensive understanding of their behaviour under shearing and compression. Consolidation and direct shear tests were conducted under various conditions to determine how the chosen material would behave within the double shear system.

2.10.3.1. Consolidation testing

The inclusion of pretension subjected the shear interfaces to compressive forces. This resulted in the eventual reduction in void space. Figure 12 highlights the infilled materials void ratio response to compressive loading over time.

Figure 12: Consolidation test of the sandy clay infilled material

2.10.3.2. Shear strength properties of the infill

The direct shear tests were conducted in two states, undrained and drained consolidation. Depending on the localised environment of the infilled material, infill in the field can present in both forms. However due to the double shear sample preparation process, all tested samples were in a state of drained consolidation. Despite this, the undrained properties were determined for comparison. During the grout curing process, moisture was drawn from the infilled material by the concrete and surrounding atmosphere.

Normal constant stress ranging from 0kPa to 500kPa were applied to the infilled samples during shearing. From plots in Figure 13a and Figure 13b the drainage condition and increasing normal pressures didn't show any over consolidation characteristics and the two test types presented slight differences to the materials shearing properties. As the normal stress was increased, the undrained samples did not plateau with the increasing displacement but continually increased throughout the entire displacement range. Conversely, the drained samples settled to a constant shear force prior to the end of the tests. The direct shear test results were then used to determine the friction angle of the infilled material in each state. It was clear that changing the drainage property of the samples resulted in sufficient changes to the friction angle of the material where the undrained samples recorded an angle of 32.2 degrees while the drained samples presented an increase of more than 7 degrees resulting in a friction angle of 39.5 degrees.

Figure 13: (a) Undrained direct shear test of infilled material; (b) Drained direct shear test of infilled material.

2.11. Fibreglass rock-bolt

The GRP bolts selected for this study were supplied by Applied Research of Australia (AROA) and were manufactured using the pultrusion method. The bolts selected for testing included the 20-tonne dowel and the 30-tonne dowel. Due to the unconventional testing method adopted throughout the double shear stage of this study, custom samples were required: both in length and thread design. As indicated in Figure 14 (top) below, the typical bolt design includes threads at only one end of the dowel as the other end remains embedded in the strata. The modified double shear testing equipment, however, required both ends of the dowel to remain exposed to allow for symmetry of the system and the application of pretension, this can be seen in Figure 14 (bottom).

Figure 14: (Top) Illustration of fibreglass bolt geometry; (Bottom) Double shear testing apparatus with double ended threads

2.11.1. Tensile test

Tensile tests were conducted on the rock bolts to determine key failure characteristics including elastic yield, plastic yield, and peak yield failure. The dowels used were the standard one-sided thread bolts. The supplied bolts did not match the required length specifications and as such were cut using a bandsaw to a length of 1.3m resulting in an exposed length of 400mm. The dowel was anchored on each end using 42mm diameter threaded metal sleeves. The base of each sleeve was sealed using a 45mm diameter metal bolt with 100mm thread. To ensure sufficient sleeve bondage, 150g of Bristar 100 expansive grout was poured into the sleeve. Due to the fast curing of the grout, the dowels were immediately but slowly inserted into the sleeve. To minimise bubble formation,

slight rotation was applied during insertion and plastic wedges were then used to ensure the dowel was centred and level. The sample was then left to cure for a minimum of six hours at which point the dowel was rotated and the same process applied to the other end. Once both sides were grouted the sample was left for a minimum of three days prior to testing. When the minimum cured period had lapsed and the sample was scheduled for testing, the exposed dowel section was wrapped in plastic to prevent debris. The samples were then secured into the testing equipment. However, due to the spiral bound design of the fibres, unravelling had the potential to negatively affect the strength properties of the dowel and as such the bolts were axially secured using a Stillson wrench. Figure 15a highlights the aggressive unravelling of the fibres during testing.

Figure 15b compared all three-rock bolt tensile results. Sample A was a 15-tonne rock bolt and was the weakest with peak values averaging 15.5kN. Sample B was a 20-tonne rock bolt and averaged 17.8 tonnes and as such achieved 89% of its designed rating. The performance of sample C or the 30-tonne rock bolt was 25.6 tonnes at 85% of its design load. The overall test variation was calculated at 6% to 18% and was considered a sufficient test quality, however, all samples failed to meet their design load. This was most likely due to variation in testing methods, testing equipment and sample preparation. The industry determined tensile properties do not indicate the exposed length of the rock bolt and as such will achieve different results.

Figure 15: (a) Tensile test post failure; (b) Tensile test comparison of 15-tonne, 20-tonne, and 30-tonne rock bolts.

2.11.2. Bending test

Bending tests were conducted using a four-point bending frame connected to the compression testing machine at the University of Southern Queensland. Tests results were inconclusive as shown in Figure 16. There was no discernible pattern of failure with each sample recording significant differences in the elastic region, plastic deformation zones, peak failure and residual loads. The only similarity evident was the gradient of the elastic region, however, this could not be confirmed as each sample recorded unique displacement ranges for this region.

Figure 16: Rock bolt four-point bending test results.

2.11.3. Punch test

The punch test was used to determine the strength properties across a small section of the dowel. The testing was conducted both parallel and perpendicular to the fibres within the dowel. To prepare the samples for the parallel punch test, the dowels were cut to a 3mm thickness perpendicular to the axis, resulting in circular samples as shown in Figure 17a. The perpendicular test samples were cut to a 3mm thickness, parallel to the axis along the centreline which resulted in the rectangular test samples shown in Figure 17b.

Once the dowels were prepared, the samples were then placed in to frame with a centre ram. The centre ram was then inserted so the sample could be aligned to ensure the ram exerts on the centre of the sample. A locking screw was then used to secure the sample in place. Once the sample had been prepared and the apparatus assembled it was aligned in the centre of the compression testing machine to ensure accurate and uniform load application. The calculations for the perpendicular tests were split into peak stress and elastic stiffness; however, the parallel tests only used the peak stress calculation. A load ratio between the perpendicular and parallel test was calculated to determine the strength variation to fibre orientation. The perpendicular failure test results indicated a failure load of approximately 13 to 14kN and so there appears to be limited correlation between the rated dowel strength and small area punch failure and no variation in failure displacement across samples. However, the elastic stiffness varied across samples. The 20-tonne rated dowels averaged a stiffness between 14.2kN/mm and 16.3kN/mm while the 30-tonne rated samples resulted in an elastic stiffness of 18.4kN/mm. These stiffness variations indicate that the 30-tonne dowel can withstand slightly greater forces prior to deformation compared to the 20-tonne samples. Similar to the perpendicular failure, the parallel punch test peak loads trend independently to dowel strength ratings with average peak loads ranging between 3.5kN and 4.1kN. By comparing the failure loads of both the perpendicular and parallel tests a ratio could be determined. Sample B and C resulted in similar load ratios with an average of 3.81, while sample A only scored 3.26. As such it was assessed that sample A was a weaker sample. Overall, the punch test was successful with only one discarded test. Sample C Test 1 was discarded due to reaching the limit of the compression tester resulting in an invalid result.

Figure 17: (a) Punch test parallel fibre sample; (b) Punch test perpendicular fibre samples.

2.11.4. Single shear test

The single shear test was conducted to identify the ultimate shear strength of the fibreglass dowels. The metal shear apparatus utilised does not reflect the failure mechanism encountered in real world applications, however the results of this test inform the calibration of the numerical simulation. All samples had a diameter of 20mm with partial threads and were cut to a length of 150mm as shown in Figure 18a.

A comparison of the peak forces for each sample indicated negligible correlation between shear strength and the samples' tensile rating. Figure 18b demonstrates similar average shear performance across rock bolts of all strengths. There does however appear to be a relationship between load rating and displacement. As the load rating increased, the failure displacement decreased as indicated by Figure 18c. The cracks found throughout the dowels appear to form parallel to the plane and could be a results of design issues with the resin. The cracked samples were tested, and it was identified there was no significant variation in results.

Figure 18: (a) Single shear fibreglass samples (b) Single shear average peak load for 15-tonne, 20-tonne, and 30-tonne samples; (c) Single shear average peak displacements for 15-tonne, 20-tonne, and 30-tonne rock bolts.

2.12. Double shear calculations

The results of the double shear tests were analysed and reduced to both material properties and overall system performance. Each test output was reported as force and displacement represented by kilonewtons and millimetres. Furthermore, the shear force data represented the overall double shear force and therefore, equation (1) reduces the data to represent the forces exerted on each plane.

$$F_{Shear\ Plane} = \frac{F_{Double\ Shear}}{2} \quad (1)$$

Where:

$F_{Double\ Shear}$: The raw test data in Newtons (N);

$F_{Shear\ plane}$: The forces isolated to the failed shear plane in Newtons (N).

Additionally, the recorded results did not outline the stresses experienced by the rock bolts at the peak shear loads. Therefore, equation (2) was used to calculate the peak shear stress and results in a value with the units of gigapascals.

$$\tau_{Stress} = \frac{F_{Shear\ plane}}{\pi r^2} \quad (2)$$

$F_{Shear\ Plane}$: the forces isolated to the failed shear plane in Newtons (N);

τ_{Stress} : the ratio between shear force and cross-sectional area in (N/m²);

r = the nominal rock bolt radius in meters (m).

3. Results and Discussions

3.1. Overview of the testing process

As discussed earlier, the testing was conducted on fibreglass rock bolts commonly used by the industry with design load capacity ratings of 20 and 30-tonnes. As a result, the double shear tests were used to identify and compare the peak strength of 20-tonne, and 30-tonne dowels in a simulated multi-shear plane environment with interfaces containing sandy clay materials. For this purpose, samples were prepared utilising a host media strength of 40MPa to simulate moderate strength rock conditions and then the fibreglass bolts were fastened using their respective nuts and washers. Due to project time constraints, long preparation times, limited number of rock bolt samples and test equipment availability, additional double shear samples couldn't be prepared for repeat test schemes and reliability testing. To simulate the complex interference of infilled shear interfaces, 5mm layers of

sandy clay fill was applied to the shear interfaces. Samples were then torqued to pretension values of 0kN, 10kN, 15kN, and 20kN. The system design properties, infill interface and rock bolt properties are outlined in Table 4.

Table 4: Rock bolt properties for infilled shear system

Unfortunately, the application of pretension was difficult to control and resulted in each sample failing to achieve the designed pretension. To minimise the variation of settled pretensions several steps were implemented. Corrections were made during the initial hour of the grout's curing process, until the grout was sufficiently set. After the initial setting stage any additional adjustments would have limited impact on the internal pretension of the system. It should be noted that some rock bolt samples experienced faster pretension settling rates than others, though by adopting the corrections, this minimised their impact on the final values. Recorded initial pretension values for all samples achieved values greater than the designed pretensions from 1kN to 2kN. As this was consistent across both the 20-tonne and 30-tonne rock bolts, testing system uniformity was maintained.

3.2. Results for 20-tonne rock bolts, double shear testing

3.2.1. Shear behaviour profile

The 20-tonne rock bolts were installed in the simulation system with applied pretensions of 0kN, 10kN, 15kN and 20kN and then tested as part of infilled discontinuities. For this, a sandy clay material of 5mm thickness was selected to replicate infilled joints. Shear loads were applied to the centre of the sample using a compression testing machine and the shear force and displacement data was simultaneously measured by internal load cells and subsequently recorded in the data logger.

Each 20- tonne sample exhibited similar shear load profiles consisting of three stages: elastic, strain-softening and failure as highlighted in Figure 19a.

The initial response to shear loading occurred within the elastic stage of the shear profile. The deformation occurring within this initial stage demonstrated elastic properties, resulting in the samples returning to their original state with no damage when the load was removed. Therefore, the rock bolts' response to loading within the elastic stage could be defined by the systems' modulus of elasticity. Continual loading resulted in the sample transitioning to the strain-softening stage. This stage was characterised by a reduced stiffness compared to that of the elastic stage and demonstrated physical indications of damage occurring within the sample as highlighted in Figure 19b. The continual application of shear load within the strain softening stage resulted in incremental increases in damage to the system. This increasing damage did not impact the rock bolts' stiffness throughout this stage and therefore the strain-softening stage could be represented by a constant stiffness value. The damage can be seen in Figure 19b, where each subsequent evidence of damage was more pronounced than the previous. The

damage could be identified by the increasing intensity of the drops in recorded shear force, culminating in a drop of approximately 10kN. The sample was able to recover and continued to progress through the stage. As the rock bolt strands experienced increasing failures, the sample eventually transitioned into the final failure stage of the profile, which was characterised by a rapid reduction in the rock bolt's ability to resist the shearing forces. The final stage was identified by the incremental decrease in the rock bolts' stiffness response. Finally, the sample was no longer able to resist any shear forces and the rock bolt subsequently experienced total failure. The peak force recorded at failure represented the culmination of shear forces, interface friction and pretension confinement.

Figure 19:(a) Example of the three failure regions for 20-tonne rock bolts with infilled shear interfaces; (b) Indication of damage to sample during strain-softening stage for the 20-tonne double shear infilled sample.

3.2.2. Pretension profile

The subsequent results were a representation of the shear forces as they transform to axial forces throughout the shearing process. The addition of infilled shear interfaces significantly altered the physical shear properties and added complexities to the shear interfaces, therefore altering how the applied shear forces transformed to axial forces. It seems that unlike the clean shear system where the interfaces were in contact as one plane, the inclusion of the infilled material increased the spacing of the interfaces from 0mm to 5mm and altered the coefficient of friction of the interface. The coefficient of friction was determined by the sandy clay infilled material as opposed to the host rock. Finally, the addition of the infilled material resulted in a doubling of the number of surfaces for each shear joint as each side of the infilled material was in contact with an interface.

It is noteworthy that the transfer of shear force to axial force was a result of failures within the grout, host rock and surface friction at the shear interface. However, for the infilled samples, the additional interfaces also influenced the transfer of shear force to axial force. The transformation of the shear forces through the host rock, grout and infilled material, in addition to the applied pretension, resulted in the infilled pretension profile illustrated in Figure 20a. Throughout the shearing process it was identified that the rock bolts' axial performance could be defined by three zones. Zone one demonstrated a linear response of almost negligible increase in axial forces to the increasing displacement. This suggested that throughout zone one there was no transformation of shear forces to axial forces and as a result the axial force resembled that of the initially applied pretension. The failure of system materials at the shear interface was a key reason for the transfer from shear force to axial force. Therefore, the lack of increase of axial force in zone one indicated that no damage was experienced at the shear interface throughout the zone. As with zone one, zone two was also represented by a linear curve profile, however,

unlike with zone one, the rock bolt recorded a significant increase in axial force. The increase in axial force from the initial pretension value of 0.75kN to approximately 1.6kN indicated that the process of shear force to axial force transformation was in progress. It was therefore inferred that damage at the interface to either the grout, host rock and/or infilled material had commenced. As the axial force increased throughout zone two with no significant spikes or dips to the recorded value, it could be assumed that there was no change to the physical integrity of the rock bolt. Zone three was the final zone of the pretension profile and was initially defined by a lack of axial force increase, zone three continued as the axial force declined. This was the result of the rock bolt no longer able to withstand increasing axial forces, indicating that the force transfer path from shear to axial had been severed, suggesting the rock bolt had experienced rupture. The axial force profile categorised by zone three ultimately is a representation of rock bolt failure throughout the axial plane.

Throughout the completion of the 20-tonne infilled testing scheme the rock bolts' axial performance trends were identified to be a result of applied pretension. With the exception of the 0kN pretension sample, all other pretensioned samples recorded peak axial forces of approximately 19kN and within 1kN of each other, as shown in Figure 20b. This suggests that although the 20-tonne rock bolts were pretensioned differently, they recorded similar peak forces. It is speculated that the 0kN sample did not achieve the same peak axial force due to the inherent differences during installation. Unlike the 10kN, 15kN and 20kN samples, the 0kN pretension sample had no initial tensioning as the sample was grouted with the rock bolt free floating as no nut installed. This was in contrast to the other samples, where their installation process required the nuts and washers to be installed and set to the required pretensions prior to grouting. This allowed the grout to set around a uniformly tensioned rock bolt. Unlike with the peak axial forces, there were incremental changes to the corresponding displacement values, highlighted in Figure 20b. Samples with lower initial pretensions recorded peak axial forces at higher displacements, such as approximately 15mm for the 0kN pretension sample in comparison to the 10kN sample recording a displacement of 14.5mm. The displacement value continued to decrease, with the 20kN sample recording the lowest displacement of 9.5mm.

Figure 20: (a) Example of pretension zones in axial force for 20-tonne rock bolt with 0kN pretension; (b) Comparison of 20-tonne infilled pretension axial force results

3.2.3. Impact of pretension on shear strength

Apart from the 20-tonne with 10kN pretension sample, the application of pretension had consistent impacts on several key properties of the 20-tonne infilled shear failure profile including the: peak shear force, failure displacement, elastic stiffness, and strain-softening stiffness. Increasing the initial pretension from 15kN to 20kN

led to an increase in the shear resistance of the rock bolts by approximately 6kN, resulting in a peak shear force of 94.2kN. However, the increase in shear response was not observed until the highest initial pretension sample of 20kN, shown in Figure 21.

Samples with the lower pretension values of 0kN and 15kN both recorded almost identical peak shear forces with a difference of 0.9kN. The 0kN pretension sample achieved a peak shear force of 89.3kN and the 15kN pretension sample achieved 87.9kN as shown in Table 5. The increase in pretension impacted the entire system as the axial forces were transferred by the grout interface, rock bolt nut and washer to the host materials. The inclusion of the sandy clay infilled material inhibited the transfer of forces to the central block like a cushion and reduced the coefficient of friction between the interfaces. Therefore, increasing the pretension of the samples facilitated efficient transformation of shear forces to axial forces resulting in higher recorded peak shear forces at higher initial pretensions. The 0kN pretension 20-tonne sample, however, did not follow to the same shear behaviours of the other samples and as a result recorded the highest peak shear value of 99.6kN, 5.4kN higher than the 94.2kN of the rock bolt with a pretension of 20kN, as shown in Figure 21 and Table 5. Unfortunately, due to time constraints, additional samples could not be manufactured to confirm the anomaly. The shear displacement recorded for each of the 20-tonne infilled samples demonstrated a proportional relationship to the sample's initial pretension. Increasing the applied pretension resulted in the samples achieving their peak shear force at lower displacement values, as shown in Figure 21, while the sample with the lowest pretension recorded the greatest displacement. Each subsequent increase resulted in an increasing reduction in the samples displacement response to shearing, where the difference between the 0kN and 10kN pretension samples was a reduction of 0.9mm. As the pretension further increased, the displacement decreased with pretensions of 10kN, 15kN and 20kN, by 1.5mm to 2.4mm. As a result, there was a total of approximately 5mm difference in the peak shear displacement values between the 0kN pretension sample and the 20kN pretension sample. Overall, the observed range of peak shear displacement, as outlined in Table 5, was between 15.3mm and 10.5mm for the 0kN and 20kN pretension samples respectively. This was in part due to the increase in confining pressures at each interface. The inclusion of the infilled material facilitated an increasingly effective transfer of the shear force from the loading ram to the shear plain interface. This meant that less energy was dissipated through points of supplementary failure, such as grout and host rock interface. As a result, the rock bolts were able to have a stiffer response throughout both the elastic and strain-softening region as outlined in Table 5.

Figure 21: Shear force and displacement comparison of all 20-tonne infilled samples.

Table 5: 20-tonne Infilled rock bolts failure properties.

The increases in pretension resulted in a significant reduction in both the intensity of the shear force dip and its duration across the displacement. During the testing of the 0kN pretension sample, the shear dip presented as a minor drop in force at a displacement of 2mm, however, reappeared four times while also changing its intensity until the final dip occurred at a displacement of approximately 11mm. The third dip presented as most significant with a change in force of 9kN occurring over a displacement of approximately 1.3mm Figure 22. Incrementally increasing the initial pretension significantly improved the shear profile of the rock bolts by reducing the impact of this phenomenon. Comparing the samples with pretensions of 0kN and 20kN, it was observed that the increased pretension had not only reduced the intensity of the spike, but also its duration, with the 20kN pretension sample recording a single dip of only 3.8kN over a displacement range of 1mm.

Figure 22: Change in recorded shear dip due to pretension increase from 0kN to 20kN for 20-tonne infilled rock bolts.

3.2.4. Failure characteristics

Upon failure, samples were dismantled and analysed for any discernible issues that may have contributed to failure or were the result of the rock bolt failure. Areas of interest included the failure angle of the rock bolt known as the hinge point, damage to material interfaces in the vicinity of the rock bolt, damages to the shear surface and structural damage within the rock bolt element. Observations were then compared across each 20-tonne infilled sample to determine the impact of pretension on the physical characteristics of the failed system. The hinge point of each sample represented the bending experienced by the rock bolt at the shear interface. As shearing was induced, the rock bolt was bent about the shear plane at the boundaries of the grout and the host rock. The rock bolt did not bend about the infilled material as the sandy clay provided no additional strength to the system. Therefore, the amount of bending experienced was determined by the strength of the rock bolt to grout and grout to host rock interfaces. Figure 23a illustrates the imprint of the hinge point caused by the rock bolt. Figure 23b highlights the resultant hinge point on the rock bolt element. With the application of pretension, additional confining pressures are added to the system materials and interfaces. Due to the compressive strength properties of the grout and host rock, the increase in pretension enabled these materials to withstand greater forces. The increase in pretension therefore reduced the bending at the hinge point as failure of the system materials occurred in compression. Table 5 further highlighted this increase in strength as the 0kN sample recorded a 15° hinge point, while the 20kN samples experienced only 10°. It is noted that this reduction in hinge point bending was not uniform with the increase in pretension. Instead, the greatest change was experienced at 10kN. No significant change to the hinge point was observed when further increasing the pretension to 15kN, in fact the angle increased

by approximately 1° . Finally, increasing the pretension to the highest setting of 20kN saw the lowest degree of hinge point rotation. The sample achieved a decrease of approximately 17% from the 15kN sample and a 33% decrease from the 0kN sample. This decrease in the bending at the hinge point resulted in an increasingly direct shearing action on the rock bolt where less forces were dissipated throughout the system and therefore the system was increasingly performing closer to a perfect shear, as highlighted in Figure 23c.

Further analysis of the samples also identified that the samples subjected to greater pretensions also suffered less damage propagating from the shear interface. When comparing the rock bolt subjected to 0kN pretension in Figure 23b and the 20kN pretension sample from Figure 23d, the 20kN sample demonstrated significantly shorter fracture propagation away from the shear interface when compared to the 0kN sample. This supported the concept that increasing the pretension has a stiffening effect on the system.

Figure 23: (a) Angle of failure and damage to grout and host rock for 20-tonne 0kN pretension infilled rock bolt sample; (b) Angle of failure and rock bolt damage for 20-tonne 0kN pretension infilled rock bolt sample; (c) Limited evidence of rotation at the hinge point for the infilled 20-tonne 20kN pretension sample; (d) Infilled 20-tonne 20kN sample demonstrating limited fracture propagation along the rock bolt element

The addition of the infilled interface resulted in failure characteristics unique to samples subjected to the infilled testing scheme. The sandy clay material selected for the infilled interface was the weakest component of the shearing system and due to the lack of confinement, it could not take advantage of the strengthening effect of pretension. Instead, the infilled interface behaved as a lubricating and cushioning material. Throughout the shearing process, the infilled material was forced through the seams of the interface. Samples with higher pretensions generated enough force on the infilled material that there were limited areas remaining intact as highlighted in Figure 24a. However, due to the disassembly process it was difficult to maintain the integrity of the infilled interface. As highlighted previously, the infilled interface provided a protective layer that prevented damage to the shear surface. Throughout the shearing process damage was subjected to the shear interface by both the formation of the hinge point as well as the splintering and final rupture of the rock bolt. With the inclusion of the sandy clay infill material, a sacrificial buffer zone was created. As the rock bolt strands failed, they came in contact with the infilled interface instead of the shear surface of the host rock. Infilled material was slowly removed preventing damage to the host material. Furthermore, as the sample failed completely, the lower coefficient of friction and the sacrificial nature of the infilled interface resulted in minimal damage to the host rocks' shear interface as the entire fractured edge of the rock bolt sheared past, highlighted in Figure 24b.

Figure 24: (a) Infilled 20-tonne 20kN sample demonstrating limited fracture propagation along the rock bolt element; (b) No evidence of scoring caused by dragging of the fractured rock bolt end on the 20-tonne 20kN infilled sample.

3.3. Results for 30-tonne rock bolts, double shear testing

3.3.1. Shear behaviour profile

Continuing with the infilled testing scheme, the 30-tonne rock bolts were tested at different pretension values with shear interfaces modified with a sandy clay infill. It was identified that the sample's failure profile was comprised of the same three regions identified in the previous test schemes of section 3.2.1, highlighted in Figure 25a. The elastic region was characterised by a linear shear response to the increase in displacement and in all samples presented as the smallest region, spanning approximately 1.5mm to 2.5mm, representing 8% to 20% of the samples' total shear displacement. Additionally, the elastic region for each sample presented as the most consistent region with the least visible variations to the recorded shear forces, further reinforcing that minimal damage has been sustained to any of the systems' components. As damage started to present, the sample transitioned into the strain-softening region. The strain-softening range alternated as the largest and second largest region, however, there was minimal correlation with pretension. The transition from the elastic region to the strain-softening region was identified by an inflection in the shear response to displacement. The inflection suggested that the rock bolt initially experienced softening as little to no load increase was recorded over approximately 0.5mm, however, then transitioned to hardening before continuing as strain-softening, as outlined in Figure 25b. The entire transition occurred over a displacement of approximately 1mm with the entire strain-softening range occupying from 36% to 52% of the shear displacement profile. The final region of each sample was the failure region, occurring when components of the system began to fail and were no longer able to withstand increasing shear forces. This region culminated in the complete failure of the rock bolt as indicated by the sudden significant drop in the recorded shear force.

Figure 25: (a) Example of the failure regions for the 30-tonne infilled rock bolt with a pretension of 0kN; (b) Example of the inflection and fluctuations in shear force for the 30-tonne sample with 10kN pretension.

3.3.2. Pretension profile

Similar to the analysis conducted on the shear curve profile, the axial forces were recorded for each test to determine the pretension profile for the 30-tonne rock bolt samples with infilled joints. Figure 26a highlights how the pretension profile was represented by three zones. The first zone represented a pre-failure state, where the

shear system was able to resist against the applied shear force. The axial force throughout zone one remained unchanged and linear with increasing displacement which indicated that no component of the shear system had begun to fail and the shear forces remained unaltered. Zone one represented a small portion of the pretension profile with the transition to zone two occurring at approximately 22% of the total displacement. Zone two was the largest component of the axial profile covering approximately 55% of the total displacement of the sample. Unlike zone one, zone two was characterised by an increasing linear force response to displacement. This indicated that during zone two, the rock bolt began loading axially due to a conversion of the shear force, additionally, the linear increase in axial force suggested that the rate of conversion was constant. Zone three was the final zone of the pretension profile and occurred at the beginning of system failure. The transition was characterised by the recorded incline in axial force reducing until a peak force was achieved. Once the sample achieved its peak value, the subsequent readings decreased for each change in displacement until the test reached completion.

Samples were tested using pretension settings of 0kN, 10kN, 15kN and 20kN, allowing the determination of the 30-tonne rock bolts' axial force characteristics. Despite the changes to the initial pretension, the samples achieved peak values of approximately 2.6 and 3.6 times the initial reading. The 20kN pretension sample had an initial axial force of 17.7kN and a peak axial force of 44.3kN Figure 26b, resulting in the peak force multiplier of approximately 2.6 times the initial value. Similarly, the 10kN sample also performed with an increase of 2.6 times the initial pretension value. The sample set to a pretension of 0.98kN failed with a peak axial force of 3.63kN, 3.6 times the initial pretension. The 15kN pretension sample on the other hand did not record any substantial increase in axial force from the initial pretension value.

Figure 26: (a) Illustration of the pretension profile zones for the 30-tonne 0kN pretension infilled sample;(b)30-tonne rock bolt infilled pretension profile comparison.

3.3.3. Impact of pretension on shear strength

Figure 27a highlights how the sample with a pretension of 0kN achieved a peak shear force of approximately 79kN, while the samples with a pretension of 10kN and 20kN reached shear forces of approximately 114kN.

In addition to the pretensions' impact on the peak shear force and displacement, the pretension also impacted the way samples transitioned from the elastic region. As shown in Figure 27b, the sample with the lowest initial pretension presented with an inflection in the shear force plot immediately after the end of the elastic region. Samples with the pretensions of 0kN, 10kN, and 15kN all demonstrated the shear force inflection response. The sample with the highest pretension, however, did not demonstrate any shear force inflection at any point after the

elastic region and continued to progress through to the next region. This was considered to be due to increased confinement pressure about the shear interfaces causing each component of the system to immediately resist the applied shear force. The inflection in the samples with lower pretensions suggested that there were less confinement forces at the shear interface. This was the consequence of the softer infilled material resulting in a portion of the shear curve flattening. As the displacement passed this inflection shear response and entered the next region, the recorded shear force resumed the typical behaviour as observed with the other tested samples. All of the 30-tonne infilled samples except for the 20kN pretension sample presented with some degree of inflection at the elastic region transition, as evident in Figure 27a. Therefore, it is suggested that a pretension of more than 15kN may be required to create a scenario where there is enough confinement on the rock bolt to facilitate a seamless transition from the elastic region. However, if the system design requires displacement flexibility to allow some displacement to occur without increasing the forces on the rock bolt, then a pretension of 15kN or less is recommended.

The application of pretension also demonstrated unique properties regarding the location of the transition thresholds between each region. As shown in Figure 27c and with the exception of the 15kN pretension sample, all other samples demonstrated near identical displacement thresholds for the transition from the elastic region, despite differences in the type of transition present. As the 15kN sample failed to meet many of the other characteristics displayed by the other samples it was assumed that the sample did not represent a typical 15kN failure. Therefore, it was concluded that pretension had no impact on the transition threshold for the elastic region. Conversely, analysing the transition to the failure region revealed that increasing the pretension resulted in an increase in both transition shear force and displacement. It was found that increasing the pretension from the 0kN sample to the 10kN sample resulted in an increase of 28% and 14% for the shear force and displacement respectively. Additionally, the increase from the 10kN pretension to the 20kN pretension saw increases of 20% for both the shear force and displacement.

Figure 27: (a) Impact of pretension on the overall shear performance of 30-tonne rock bolts with infilled shear interfaces; (b) Impact of pretension on the elastic to strain-softening region for 30-tonne rock bolts tested with infilled shear joints; (c) The effect of pretension on the elastic region transitions for the 30-tonne rock bolts with infilled joints.

3.3.4. Failure characteristics

Like the previous samples tested with the infilled testing scheme, the samples were analysed for the following properties: hinge point, shear interface damage and rock bolt element damage. The utilisation of pretension

resulted in recordable changes to the appearance of the hinge point. As the pretension increased, so did the angle of the hinge point from 9° to 11.5° for the 0kN and 10kN pretension samples respectively and then to 12° for the 20kN pretension sample. The 0kN and 20kN samples were displayed in Figures 28a and 28b, as they best highlighted the described changes to the hinge point. The incremental changes to the hinge point are due to the change in confinement pressure at the shear interface. When the pretension was increased, greater pressures were imparted to the shear surface, resulting in the bending of the rock bolt occurring over a shorter length of the bolt and therefore forming hinge points of greater angles. Another characteristic that was evidently altered by increasing the pretension was the extent to which damage propagated through the rock bolt away from the shear interface. With each increase in pretension, it was found that the extent of damage propagation decreased. The differences in damage propagation of the 20kN and 0kN pretension samples are highlighted in Figures 28b and 28c.

The presence of damage propagation was closely related to the bending experienced at the hinge point. Samples with smaller hinge point angles experienced greater damage propagation as opposed to samples with larger hinge point angles. The correlation with the hinge point and pretension is most likely due to the material properties of fibreglass. Fibreglass typically responds poorly to forces that induce bending, generally resulting in crack formations and fibre/resin delamination. This was evident in the tested samples where the increase in pretension reduced the length of the rock bolt that experienced bending. Additionally, increasing the pretension meant that the fibreglass experienced more direct shearing and therefore the internal strands were severed either at or close to the shear plane before there was a chance for cracks to propagate.

Figure 28: (a) Angle of failure for 30-tonne rock bolt with 0kN pretension with infilled shear conditions; (b) Angle of failure and damage propagation for 30-tonne rock bolt with 20kN pretension with infilled shear conditions; (c) Damage propagating through element for 30-tonne rock bolt with 0kN pretension with infilled shear conditions.

3.4. Comparison between 20-tonne and 30-tonne rock bolts

3.4.1. Shear behaviour profile

The following comparative analysis outlines the similarities and differences between the shear performance of the 20-tonne and 30-tonne rock bolt types. When analysing the shear profile for each rock bolt type as highlighted in Figure 29a, it was evident that the 20-tonne and 30-tonne rock bolts with infilled shear discontinuities, presented with similar failure responses. The similarities in failure responses could be attributed in part to the similarities in the fibreglass properties of the two rock bolt types. As demonstrated in Figure 29a the samples exhibited similar

shear profile characteristics such as the inflection present at the transition from the elastic region. However, the presence of the inflection was not mirrored for each rock bolt type. It was identified that the 30-tonne samples with a pretension of 20kN did not exhibit any inflection at the elastic transition. Figure 29b demonstrated that the 20-tonne samples retained the inflection properties from samples with lower pretensions. This indicated that the added strength of the 30-tonne rock bolt sample and the pretension of greater than 15kN may be required to overcome the shear interface weakness resulting from the infilled shear joints. In addition to the difference of the elastic region, compared samples also demonstrated differences regarding the displacement duration of the failure region. It was found that the 20-tonne infilled samples presented with a failure region occurring over a shorter displacement range when compared to the 30-tonne samples. Figure 29b highlighted that the 30-tonne rock bolt with a pretension of 20kN recorded a failure region over approximately 8.5mm as opposed to 2.5mm for the 20-tonne sample with the same pretension. The displacement ranges fluctuated across all samples, preventing clear correlation with pretension, although the 30-tonne samples recorded longer failure range displacements. Figure 29a also highlighted an increase of 2.2mm in the 30-tonne's failure displacement range compared to the 20-tonne's failure region when comparing samples with 10kN pretension. It was however evident that between the 20-tonne and 30-tonne samples the failure region commenced at similar displacements. The longer displacement range for the 30-tonne rock bolts may be attributed to the material properties of the rock bolt as well as the compressive strength of both the grout and the concrete. These components experienced increased forces due to the additional strength of the 30-tonne samples. These forces have the potential to cause internal failures within the grout and concrete resulting in greater forces being transferred over a longer duration before culminating in rock bolt failure.

Figure 29: (a) Shear profile comparison of 10kN pretension 20-tonne and 30-tonne rock bolts with infilled Interfaces; (b) Comparison of the elastic region transition and the failure region of the 20kN pretension 20-tonne and 30-tonne rock bolts with infilled shear planes

Both rock bolt types demonstrated no correlation between peak shear force and applied pretension, with the 20-tonne samples performing within a consistent range of 88kN to 100kN as shown in Table 6. The 30-tonne samples also showed no correlation between shear force and pretension, although the samples demonstrated significant shear force variability with a performance ranging from 69kN to 114kN. The lowest performing samples were the 0kN and 15kN pretension samples Table 6. This indicated that despite the shear forces transferring to axial forces during the shearing process, there was no mechanism for the reverse to occur. Additionally, pretension didn't indicate any shear strengthening properties.

Unlike with the shear force however, the 20-tonne samples demonstrated a clear correlation between the applied pretension and the peak failure displacements. As the pretension increased, the displacement at which failure occurred decreased incrementally. The initial 0kN sample failed at 15.3mm and the final 20kN sample failed at just 10.6mm as highlighted in Table 6. However, this trend was not evident with the 30-tonne sample. The 30-tonne samples showed no correlation between the initial pretension and the displacement at failure. Both the 0kN and 20kN samples failed within 1mm of each other and the 15kN sample presented as a potential outlier due to its 5mm to 6mm lower peak displacement. Additionally, the total displacement difference between the 0kN and 20kN samples was also just 1mm.

Table 6: Summary of peak forces and shear stresses of all infilled samples

3.4.2. Pretension profile

The pretension profile was analysed and compared across all tested infilled samples. While there were variations in the peak displacements and peak axial forces, all samples followed the same three zone profile outlined in sections 3.2.2 and 3.3.2. Each of the samples progressed through the same zones throughout shearing beginning with zone one represented by the initial flat section of the curves. During this section each sample maintained the initial pretension value and experienced no increase in axial force. This suggested that there was no internal conversion of the shearing force to axial force. The key difference in the case of the 0kN pretension samples was that the 30-tonne sample-maintained zone one over a shorter displacement range, approximately 50% of the 20-tonne samples', as illustrated in Figure 30. This could be attributed to the extra strength of the 30-tonne sample resulting in earlier internal damage that could facilitate the transition from shear force to axial force.

Conversely, it was also observed that the 30-tonne samples-maintained zone two for a longer displacement when compared to the 20-tonne samples. As zone two was where a majority of the shear forces were converted to axial forces, the increased duration of this zone for the 30-tonne samples also resulted in the 30-tonne samples achieving higher axial forces. Figure 30 also demonstrated that the additional duration of zone two resulted in greater axial forces. Zone three, however, remained consistent across all samples. Zone three encompassed the failure portion of the rock bolt and as all samples were comprised of similar fibreglass, the failure mechanism of the core materials in the rock bolt remained constant. It was not possible to compare displacements of zone three as this was heavily influenced by the completion of the testing process. Hence, the zone three displacement was dependent on the point in time when the equipment detected failure and stopped applying shear. Despite significant variations to the recorded peak axial forces, in the case of the 30-tonne sample with 0kN pretension, the sample experienced more than double the axial force of the 20-tonne sample with 0kN pretension. The overall peak axial forces were

influenced by the rock bolts' performance in zone two. When samples reached the zone three failure stage of the profile, only a minor increase in axial force was recorded before the samples quickly lost the ability to resist shear displacements.

Figure 30: Comparison of the axial force profile for both 20-tonne and 30-tonne 0kN pretension samples with infilled shear planes

3.4.3. Impact of pretension on shear strength

The differences to the applied pretension were recorded in Table 4. Both rock bolt types presented with different responses to the applied pretensions with their performance summary outlined in Table 6. The application of pretension had the greatest consistent impact on the performance of the 20-tonne rock bolts, despite the 30-tonne rock bolts recording the greatest changes. The increase from 0kN pretension to 10kN pretension saw a gradual increase of 11% for the failure shear force of the 20-tonne sample while the 30-tonne sample recorded an increase of 45% as evidenced in Figure 31a. Both rock bolt types recorded similar magnitude of change to their failure displacement response, however, the 30-tonne samples recorded an increase of 3% in its failure displacement, while the 20-tonne samples recorded a decrease of 4%. This was due to the 20-tonne sample's inherent weaker strength. The addition of the pretension incrementally increased the strength of the system components due to increased confinement and as such, reduced the rock bolt's ability to resist shear displacement. On the other hand, the 30-tonne rock bolts were inherently stronger than the 20-tonne rock bolts and as a result were under-utilised in scenarios with lower pretensions. This was evident through the significant increase in shear force resistance and the increase in the failure displacement between the 0kN and 10kN samples. The 30-tonne rock bolt however, did not perform consistently with the increase to a pretension of 15kN, which saw a decrease in both failure shear force and failure displacement. This could be the result of a faulty sample as well as the strength of the rock bolt being an ineffective match to the test system's design. Poorly matching of a rock bolt type to the environment could result in inefficient transfer of forces through the element. The inefficient transfer of forces could present as a decrease in overall rock bolt performance, despite the greater design strength of the rock bolt. In this situation of small-scale testing, an over strengthened rock bolt could divert shear force to continually damage components within the system and can be characterised by an extended failure region. This could also result in increased bending within the element, reducing its effective strength due to the poor bending properties of the intrinsic fibreglass matrix.

Similarly, the rock bolts' response to an increase from 0kN pretension to 10kN both samples exhibited similar trends when increasing the pretension from 15kN to 20kN as shown in Figure 31b. The 20-tonne samples recorded

an increase in the failure shear force of 7% with an overall increase of 5.5% from the 0kN sample to the 20kN sample. The 20-tonne samples also maintained a consistent decrease in failure displacement with a decrease of 20% between the 15kN and 20kN samples. The 20-tonne sample recorded an overall decrease of 30% in its failure displacement when comparing the 0kN and 20kN samples. The 30-tonne samples also maintained their performance with variable failure shear forces and failure displacements. Increasing the pretension from 15kN to 20kN saw similarly large changes in shear failure forces with an increase of 40%. This was due to the 15kN sample performing significantly lower than the other samples. In a similar manner the failure displacement also recorded an increase of 50% for the same reason. Overall, the 30-tonne sample recorded a significant 45% increase in failure shear force when comparing the samples of the extreme ends of the pretension scale of 0kN and 20kN. Interestingly, the 30-tonne sample only recorded an increase in 6% for the failure displacement further reinforcing its variable performance. Finally, it was found that overall, the increase in pretension had a more significant impact on the 20-tonne rock bolts' failure displacement performance, while the 30-tonne sample experienced a greater impact on its peak shear force.

Figure 31: (a) Influence of pretension increase from 0kN to 10kN on shear force for 20-tonne and 30-tonne rock bolts with infill joints; (b) Influence of pretension increase from 15kN to 20kN on shear force for 20-tonne and 30-tonne rock bolts with infill joints.

3.4.4. Failure characteristics

Sections 3.2.4 and 3.3.4 provide a detailed analysis of the failure characteristic of each rock bolt and highlighted three key components of failure: the hinge point, the rock bolt structural damage and the shear surface damage.

Unlike the clean interface samples, both the 20-tonne and 30-tonne rock bolt infilled interface shear samples experienced different degrees of bending when the hinge points were analysed.

At a pretension of 0kN, the 20-tonne experienced a greater degree of bending by approximately 6° , when compared to the 30-tonne rock bolt as shown in Figure 32a. Furthermore, both rock bolt types exhibited different responses to the increase in pretension. The 20-tonne rock bolts recorded a decrease to the degree of bending when pretension was increased from 0kN. On the other hand, the 30-tonne rock bolts recorded an increase to the amount of bending experienced at the same change in pretension.

Failure differences were also recorded when analysing the condition of the rock bolt element post failure. With a pretension of 0kN the 20-tonne rock bolt experienced a significant amount of damage propagating along the rock bolt away from the shear interface. This failure was only partially present on the 30-tonne rock bolt samples, with the rock bolt experiencing damage on one half of the shear interface as shown in Figure 32b.

Neither rock bolt recorded shear interface gouging thanks to the lubricating effects of the sandy clay infill. The 20-tonne rock bolt however, experienced damage at the shear interface at 0kN as a result of the greater hinge point bending. In comparison the 30-tonne rock bolt recorded little to no damage to the shear interface due to the lower degree of bending as shown in Figure 32c. Additionally, at low pretension settings, the infilled material did not fill all the shear interface voids for either of the 20-tonne and 30-tonne rock bolts as seen in Figure 35c.

Figure 32: (a) Comparing rock bolt structural damage for 20-tonne and 30-tonne rock bolts with 0kN pretension and infilled shear interfaces; (b) Representation of rock bolt damage for 30-tonne rock bolt with infilled shear interfaces and 0kN pretension; (c) Comparing shear plane damage of 20-tonne and 30-tonne rock bolts with infilled shear interfaces and 0kN pretension

Increasing the pretension to 20kN resulted in two opposite failure trends for the 20-tonne and 30-tonne rock bolts. As the pretension was increased, the 20-tonne rock bolts experienced a reduction in the severity of bending at the hinge point, while the 30-tonne rock bolt recorded an increase in bending when compared to the 0kN samples. Despite this difference, the 20-tonne and 30-tonne rock bolts experienced similar amounts of bending with 20kN of pretension. The similar magnitudes of bending at the hinge point resulted in the two rock bolts experiencing similar degrees of damage propagating from the shear plane as shown in Figure 33a.

Figure 33 shows that despite increasing the pretension to 20kN, neither the 20-tonne or 30-tonne samples experienced damage to the shear interface. The infilled material behaved as a protective barrier to the shear interface. Additionally, increasing the pretension resulted in more of the voids on the shear surface being filled by the infill material as shown in Figure 33b.

Figure 33: (a) Comparing rock bolt hinge point and rock bolt damage for 20-tonne and 30-tonne rock bolts with 20kN pretension and infilled shear interfaces; (b) Comparing shear plane damage of 20-tonne and 30-tonne rock bolts with 20kN pretension and infilled shear interfaces.

Upon evaluating the shear profile for each sample, it was found that all samples followed a three-part failure profile comprised of an elastic region, strain-softening region and failure region. Additionally, it was found that the infilled shear planes had no impact on the overall shear profile of the 20-tonne and 30-tonne rock bolts. While samples experienced some common responses to shearing, including the three-stage pretension failure profile, applying pretension also resulted in unique shearing properties for the 20-tonne and 30-tonne samples. Unlike the 20-tonne samples, 30-tonne rock bolt samples with a 15kN pretension or less recorded an inflection at the transition from the elastic region of the shear profile. Increasing the pretension past 15kN saw the elimination of this inflection. When comparing the physical failure characteristics of the samples, it was found that the increase

in pretension incrementally increased the angle experienced at the hinge point. Finally, as the pretension was increased, less damage propagating down the rock bolt element was evident.

4. Conclusion

In this paper, the shear performance of the fibreglass rock bolts with infilled shear interfaces has been investigated by conducting the infilled joint test scheme. For this purpose, the double shear testing apparatus was modified to address the issues and shortcomings of the established testing methodology. The modified testing apparatus provided new insights to the shear behaviour properties of fibreglass rock bolts while also minimising the limitations encountered by previous studies. Also, the test scheme and equipment were designed to allow for the testing of additional system parameters simultaneously while subjecting shear forces. This allowed the testing apparatus to monitor the rock bolts axial response to shearing but also to examine the influence changes to the system's conditions can have on the overall performance of the rock bolts. To ensure a comprehensive study, experiments were also subjected to various system properties. These properties included fibreglass rock bolts of 20-tonne and 30-tonne tensile ratings and pretensions of 0kN, 10kN, 15kN and 20kN. Great care was taken during sample preparation to ensure sample uniformity, however, achieving the specified pretensions proved to be a difficult task. Variability in the rock bolts' quality resulted in several discarded bolts during assembly and one discarded test sample. The infilled test scheme was conducted with 5mm thick sandy clay infilled shear interfaces. It was found that all tested infilled samples experienced the three-part failure profile comprised of the elastic, strain-softening and failure regions. Several exclusive shear behaviour characteristics were identified during the infilled test scheme. Firstly, both rock bolt types experienced a decrease to the shear failure displacement. The 20- tonne rock bolts experienced the greatest overall decreases. Contrastingly, the infilled shear system registered successive increases to the shear failure forces, with the 30- tonne samples experiencing the greatest overall increases. Secondly, there was a notable increase in the shear force performance of 30-tonne rock bolts over the 20- tonne bolts. The 30-tonne rock bolts also showed strong correlations between increasing the pretension setting and decreasing failure displacement. Finally, both the 20-tonne and 30-tonne rock bolts experienced incremental increases to the hinge point angle with each pretension setting increase. Completing this research study brought attention to several areas of possible investigation to both the designed test schemes and new areas of study that were not explored within the scope of this research. Infilled test schemes used in this research could be extended to test additional aspects of rock bolt performance. Due to high variability in the rock formation processes, it would be highly valuable to study the impact of varying degrees of infilled asperities and variations to the material properties of the infill and its thickness

Declaration of competing interest

The authors declare that they have no known competing financial interests or personal relationships that could have appeared to influence the work reported in this paper.

Data Availability

Data generated or analysed during this study are available from the corresponding author upon reasonable request.

Acknowledgements

Authors would like to acknowledge the in-kind support of MINOVA and Jenmar Australia, and in particular Mr Robert Hawkers and Dr Peter Craig for this research study.

5. References

2009. BS 7861. Strata reinforcement support system components used in coal mines -Part 1: Specification for rockbolting and Part 2: Specification for Flexible systems for roof reinforcement.: BSI.
- Aziz N., Pratt D., and Williams, R. (2003). Double Shear Testing of Bolts. In: AZIZ, N. (ed.) Coal Operators' Conference. Wollongong: The University of Wollongong.
- Aziz, N., Craig, P., Nemcik, J., and Hai, F.I. (2013a). Rock bolt corrosion – an experimental study. In: AZIZ, N. (ed.) Coal Operators' Conference Wollongong: The University of Wollongong.
- Aziz, N., Craig, P., Nemcik, J., and Hai, F.I. (2013b). Rock bolt corrosion – an experimental study. In: AZIZ, N. (ed.) Coal Operators' Conference. Wollongong: The University of Wollongong.
- Aziz, N., Craig, P., Mirzagherbanali, A., Rasekh, H., Nemcik, J., and Li, X. (2015a). Behaviour of Cable Bolts in Shear; Experimental Study and Mathematical Modelling. In: AZIZ, N. (ed.) 15th Coal Operators' Conference Wollongong: University of Wollongong.
- Aziz, N., Gilbert, D., Nemcik, J., Mirzagherbanali, A., and Burton, R. (2015b). The Strength properties of Fiber glass and other polymer based Dowels for Strata Reinforcement in Coal mines. Third Australian Ground Control in Mining Conference. Sydney, Australia: Ausimm.
- Aziz, N., Mirzagherbanali, A., Nemcik, J., Rasekh, H., Li, X. (2016). A Follow up to Study the Behaviour of Cable Bolts in Shear: Experimental Study and Mathematical Modelling. In: AZIZ, N. (ed.) 16th Coal Operators' Conference. Wollongong: University of Wollongong.
- Aziz, N., Rink, O., Rasekh, H., Hawkins, E., Mirzagherbanali, A., Yang, G., Khaleghparast, S., Mills, K., Jan, N., and Li, X. (2017). Single shear testing of various cable bolts used in Australian mines. In: AZIZ, N. (ed.) 17th Coal Operators' Conference. Wollongong: University of Wollongong.

- Barton, N. (1971). A relationship between joint roughness and joint shear strength. *Mecanique des Roches*. Nancy, France: Symposium Soc. Internat.
- Barton, N. (1973). A review of the shear strength of filled discontinuities in rock. *Bergmekanikk*. Oslo, Norway.
- Chang, X., Wang, G., Liang, Z., Yang, J., and Tang, C. (2017). Study on grout cracking and interface debonding of rockbolt grouted system. *Construction and Building Materials* 135: 665-673.
- Clifford, B., Kent, L., Altounyan, P., and Bigby, D. (2001). Systems Used in Coal Mining development in Long Tendon Reinforcement. 20th International Conference on Ground Control in Mining. West Virginia, USA.
- Conway, C. C. (1948). Roof support with suspension rods. *Proceedings of the Illinois Mining Institute*. Springfield, Illinois: Mining Electrical Group.
- Oliveira, D., and Indraratna, B. (2010). Comparison between models of rock discontinuity strength and deformation. *Journal of Geotechnical and Geoenvironmental Engineering* 136: 10.
- Forbes, B., Vlachopoulos, N., Diederichs, M.S., and Aubertin, J. (2020). Augmenting the in-situ rock bolt pull test with distributed optical fiber strain sensing. *International Journal of Rock Mechanics and Mining Sciences* 126: 104202.
- Frketic, J., Dickens, T., and Ramakrishnan, S. (2017). Automated manufacturing and processing of fiber-reinforced polymer (FRP) composites: An additive review of contemporary and modern techniques for advanced materials manufacturing. *Additive Manufacturing* 14: 69-86.
- Gilbert, D., Mirzaghobanali, A., Li, X., Rasekh, H., Aziz, N., and Nemcik, J. (2015). Strength Properties of Fibre Glass Dowels Used for Strata Reinforcement in Coal Mines. In: AZIZ, N. (ed.) *Coal operators' Conference*. Wollongong: University of Wollongong.
- Hartman, W., and Hebblewhite, B. (2003). Understanding the performance of Rock Reinforcement Elements under Shear Loading through Laboratory Testing - A 30-year History. 1st AGCM Conference.
- Hassell, R., Villaescusa, E., Thompson, A., and Kinsella, B. (2004). Corrosion assessment of ground support systems. In: VILLAESCUSA, E. and POTVIN, Y. (eds.) *Ground Support in Mining and Underground Construction*. London: Taylor and Francis Group, London.
- Jahangir, E., Blanco-Martin, L., Hadj-Hassen, F., and Tijani, M. (2021). Development and application of an interface constitutive model for fully grouted rock-bolts and cable-bolts. *Journal of Rock Mechanics and Geotechnical Engineering* 13: 811-819.

- Jodeiri Shokri, B., Entezam, S., Nourizadeh, H., Motallebian, A., Mirzaghobanali, A., McDougall, K., Aziz, N., and Karunasena, K. (2023). The effect of changing confinement diameter on axial load transfer mechanism of fully grouted rock bolts. In: AZIZ, N. (ed.) 2023 Resource Operators Conference. Wollongong: University of Wollongong 290-295.
- Li, X., Aziz, N., Mirzaghobanali, A., and Nemicik, J. (2016). Behavior of Fiber Glass Bolts, Rock Bolts and Cable Bolts in Shear. *Rock Mechanics and Rock Engineering* 49: 2723-2735.
- Li, F., Quan, X., Jia, Y., Wang, B., Zhang, G., and Chen, S. (2017a). The Experimental Study of the Temperature Effect on the Interfacial Properties of Fully Grouted Rock Bolt. *Applied Sciences* 7: 327.
- Li, X., Aziz, N., Mirzaghobanali, A., and Nemicik, J. (2017b). Comparison of the shear test results of a cable bolt on three laboratory test apparatuses. *Tunnelling and Underground Space Technology* 61: 82-89.
- Maranan, G., Manalo, A., Karunasena, K., and Benmokrane, B. (2015). Bond Stress-Slip Behavior: Case of GFRP Bars in Geopolymer Concrete. *Journal of Materials in Civil Engineering* 27: 04014116.
- Mark, C. (2017). Design of roof bolt systems. In: LABOR, U. S. D. O. (ed.). Pittsburgh, PA: Pittsburgh Research Laboratory.
- Mirzaghobanali, A., Nemicik, J., and Aziz, N. (2014). Effects of cyclic loading on the shear behaviour of infilled rock joints under constant normal stiffness conditions. *Rock Mechanics and Rock Engineering* 47:1373-1391.
- Mirzaghobanali, A., Rasekh, H., Aziz, N., Yang, G., Khaleghparast, S., and Nemicik, J. (2017). Shear strength properties of cable bolts using a new double shear instrument, experimental study, and numerical simulation. *Tunnelling and Underground Space Technology* 70: 240-253.
- Mirzaghobanali, A., Gregor, P., Alkandari, H., Aziz, N., and McDougall, K. (2018). Mechanical behaviours of grout for strata reinforcement. *Coal Operators Conference (ROC2018): The University of Wollongong* 373-377.
- Mirzaghobanali, A., Ghirmire, B., Rastegarmanesh, A., Nourizadeh, H., McDougall, K., and Aziz, N. (2022). Shear behavior of clayey infilled rock joints having triangular and sinusoidal asperities, in Naj Aziz and Bob Kininmonth (eds.), *Proceedings of the 2022 Resource Operators Conference, Mining Engineering, University of Wollongong*, 18-20.
- Nemicik, J., Gale, W.J., and Fabjanczyk, M.W. (2006). Methods of Interpreting Ground Stress Based on Underground Stress Measurements and Numerical Modelling In: AZIZ, N. (ed.) *Coal Operators' Conference Wollongong: University of Wollongong*.

- Nourizadeh, H., Mirzaghobanali, A., Aziz, N., McDougall, K., Jodeiri Shokri, B., Sahebi, A.K., Motallebiyan, A., and Entezam, S. (2023). Finite element numerical modelling of rock bolt axial behaviour subject to different geotechnical conditions. In: AZIZ, N. (ed.) 2023 Resource Operators Conference. Wollongong: University of Wollongong 221-229.
- Rajapakse, R. (2016). 33 - Rock bolts, dowels, and cable bolts. In: RAJAPAKSE, R. (ed.) Geotechnical Engineering Calculations and Rules of Thumb (Second Edition). Butterworth-Heinemann.
- Song, M.K., Choo, S.Y., Kang, S.S., and Cho, Y.D. (2008). A Comparison for shear resistant behavior of joints with rock and spiral bolts installed-a numerical approach. *Geosystem Engineering* 11: 57-62.
- Spearing, A., Mondal, K., and Bylapudi, G. (2010) The corrosion of rock anchors in US coal mines. SME, Annual Meeting. Phoenix: SME.
- Thompson, A., and Villaescusa, E. (2014). Case studies of rock reinforcement components and systems testing. *Rock Mechanics and Rock Engineering* 47: 1589-1602.
- Thenevin, I., Blanco-Martin, L., Hadj-Hassen, F., Schleifer, J., Lubosik, Z., and Wrana, A. (2017). Laboratory pull-out tests on fully grouted rock bolts and cable bolts: Results and lessons learned. *Journal of Rock Mechanics and Geotechnical Engineering* 9: 843-855.
- Vandekraats, J.D., and Watson, S.O. (1996). Direct Laboratory tensile testing of select yielding rock bolt systems, New Mexico, United States. Department of Energy.
- Waclawik, P., Ram, S., Kumar, A., Kukutsch, R., and Mirek, A. (2019). Field and simulation study for rock bolt loading characteristics under high stress conditions. In: AZIZ, N. (ed.) 19th Coal Operators' Conference Wollongong: University of Wollongong.
- Windsor, C., and Thompson, A. (1992). Reinforcement design for jointed rock masses. Proceedings of the 33rd US Symposium on Rock Mechanics.
- Windsor, C.R. (1997). Rock reinforcement systems. *International Journal of Rock Mechanics and Mining Sciences* 34: 919-951.

Table1: Experimental plan for reinforced concrete blocks with infilled joints

Dowel (Tone)	Pretensions (KN)
20	0
	10
	15
	20
30	0
	10
	15
	20

Table 2: UCS test results of the concrete used for double shear casting

Sample	Pressure (MPa)	Load (kN)
1	29.10	228.7
1.3	52.65	413.3
2	50.50	396.6
3	55.90	438.8
4	50.90	400.0
6	59.40	466.8
7.1	83.76	657.5
7.2	61.50	482.9
8	78.85	619.0
9	67.50	529.7
Average	47.81	375.48

Table 3: Brazilian testing of concrete used for double shear casting

Sample	Pressure (MPa)	Load (kN)
1.2	5.20	163.0
1.4	4.30	133.8
2	3.53	110.9
3	5.15	161.7
4	5.00	157.6
5	4.76	149.5
7.1	3.52	110.6
7.2	5.40	169.7
7.3	5.10	159.0
Average	4.70	146.2

Table 4: Rock bolt properties for infill shear system

Bolt Type	Rock bolt Diameter (mm)	Design Shear Capacity (t)	Designed Pretension (kN)	Applied Pretention (kN)	Tested Pretension (kN)	Infill Thickness (mm)	Rate of Loading (mm/min)
20T0kN Infill	20	20	0	1.5	0.75	5	1
20T10kN Infill	20	20	10	12	12.39	5	1
20T15kN Infill	20	20	15	17	14.35	5	1
20T20kN Infill	20	20	20	22	19.65	5	1
30T0kN Infill	20	30	0	1.6	0.98	5	1
30T10kN Infill	20	30	10	12	10.35	5	1
30T15kN Infill	20	30	15	17	15.89	5	1
30T20kN infill	20	30	20	21	17.71	5	1

Table 5: 20-tonne Infilled rock bolts failure properties.

Bolt Type	Failure Displacement (mm)	Peak Shear Force (kN)	Elastic Stiffness (kN/mm)	Strain-softening Stiffness (kN/mm)	Hinge Point (°)
20T0kN Infill	15.3	89.3	10.9	5.1	15
20T10kN infill	14.4	99.6	16.8	5.9	11
20T15kN Infill	12.9	87.9	14.6	6.0	12
20T20kN Infill	10.5	94.2	26.5	6.9	10

Table 6: Summary of peak forces and shear stresses of all infilled samples

Bolt type	Peak shear force (kN)	Displacement at peak shear (mm)
20T0kNInfill	89.3	15.3
20T10kNInfill	99.6	14.7
20T15kNInfill	87.9	12.8
20T20kNInfill	94.2	10.6
30T0kNInfill	78.5	17.3
30T10kNInfill	113.9	17.8
30T15kNInfill	68.8	12.2
30T20kNInfill	114.1	18.3



Figure 1: Outline of SANS Machine used for double shear testing

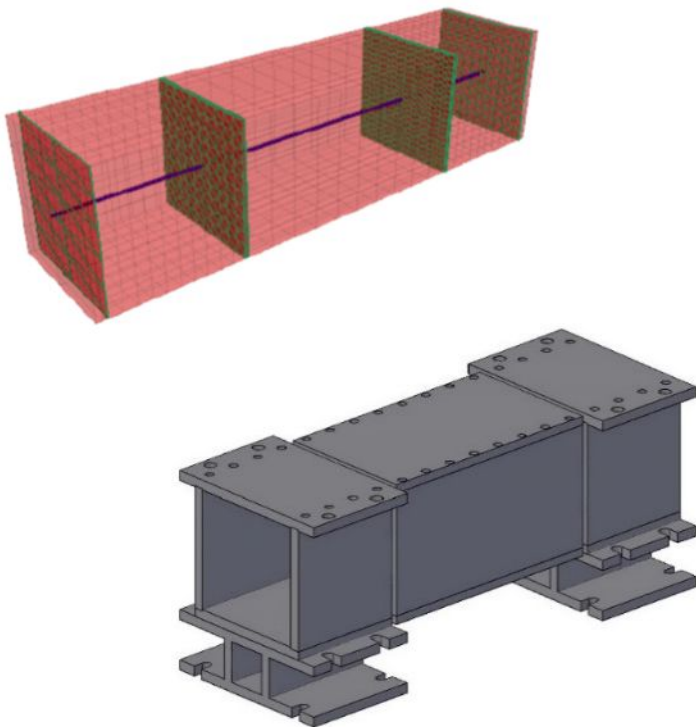


Figure 2: MK1.5 Double shear box design

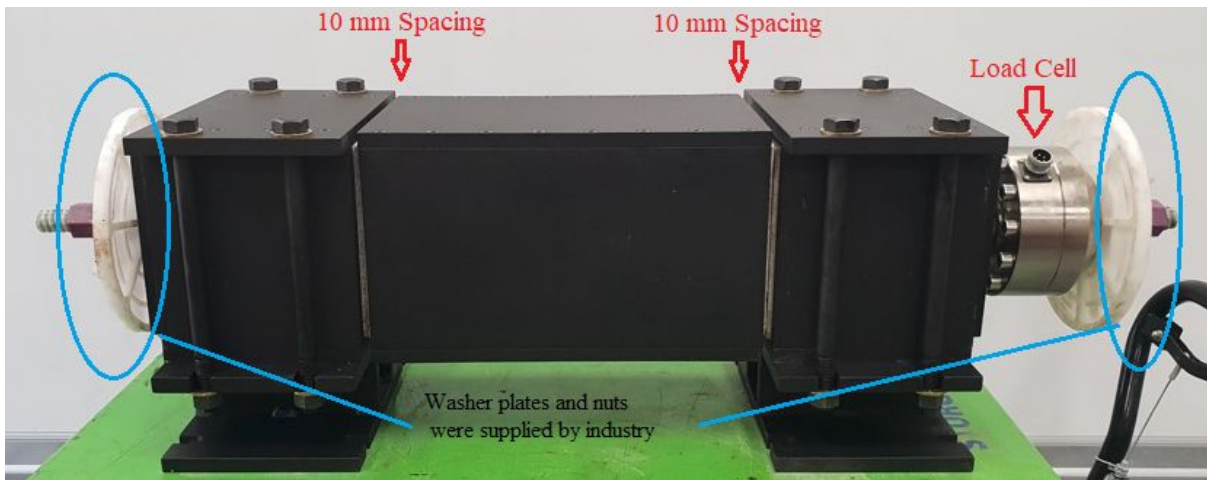


Figure 3: Assemble double shear apparatus highlighting key features such as 10mm spacing at each interface

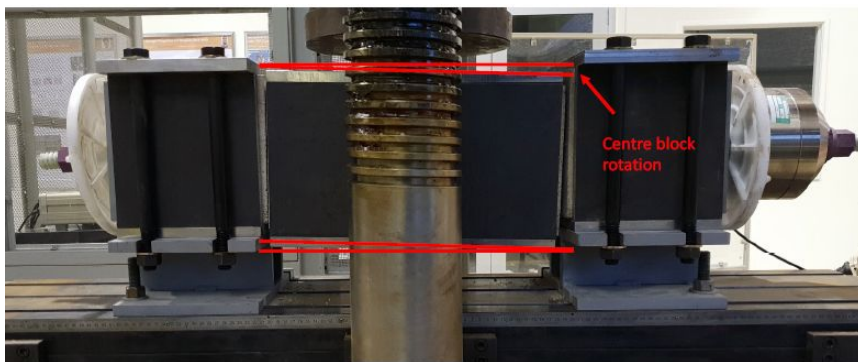


Figure 4: Centre block rotation because of testing

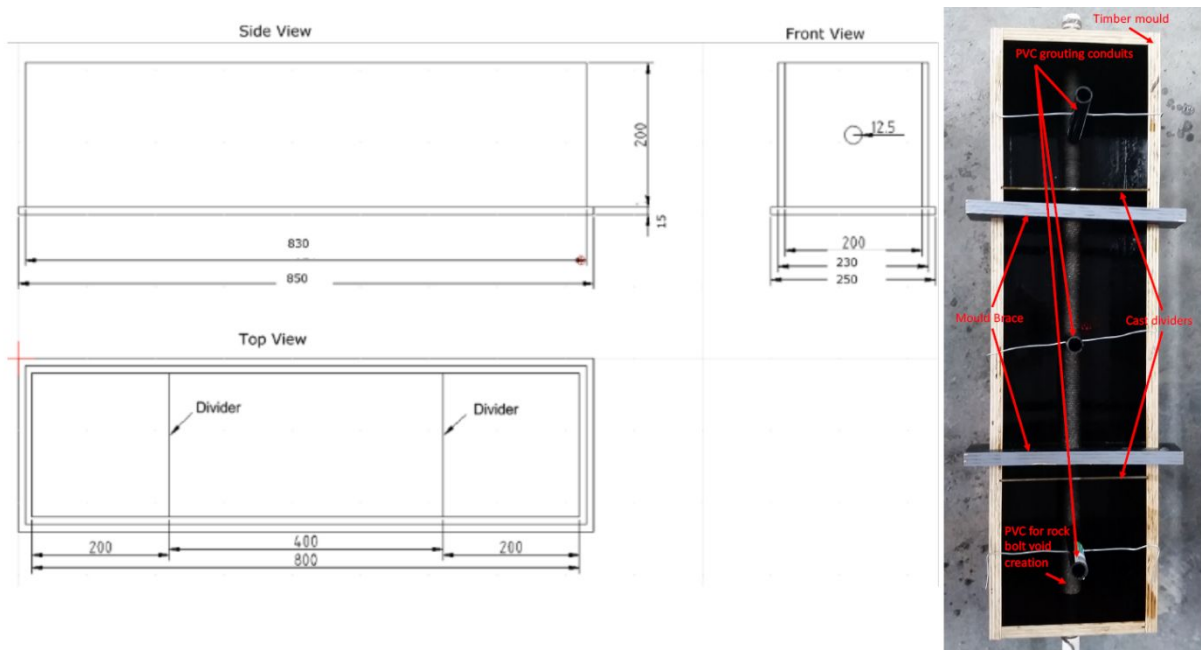


Figure 5: (a) Double shear mould design and key features.



Figure 6: Severe damage resulting from a weak concrete matrix.

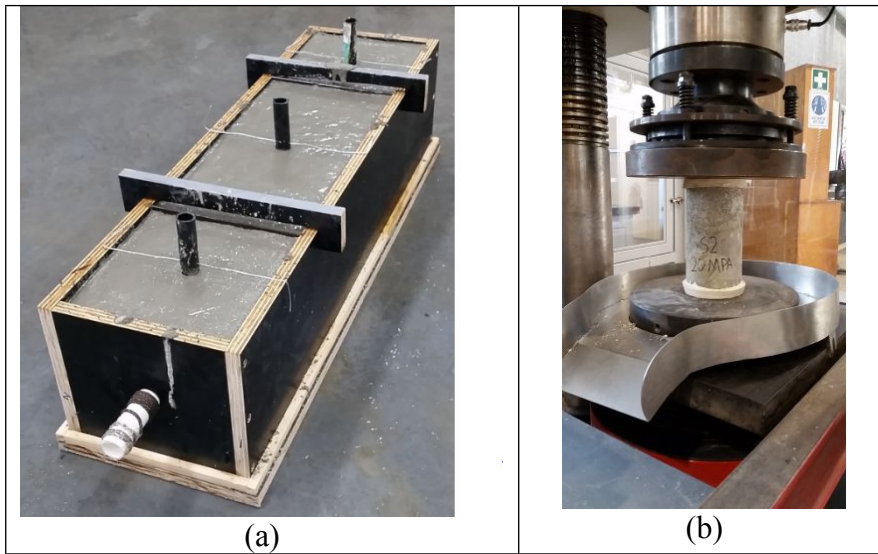


Figure 7: (a) Cast of double shear sample; (b) Cylindrical concrete samples for UCS testing

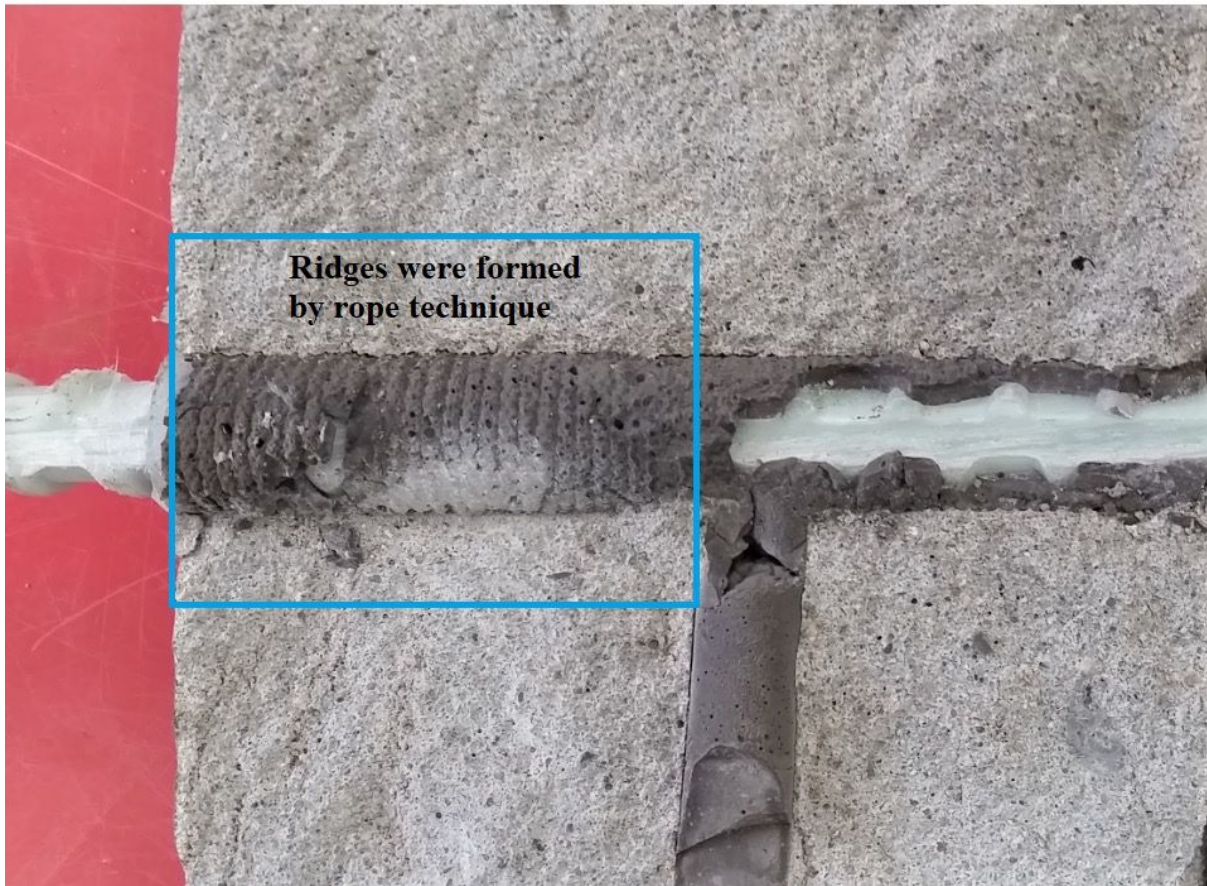


Figure 8: Grouting quality examination after testing

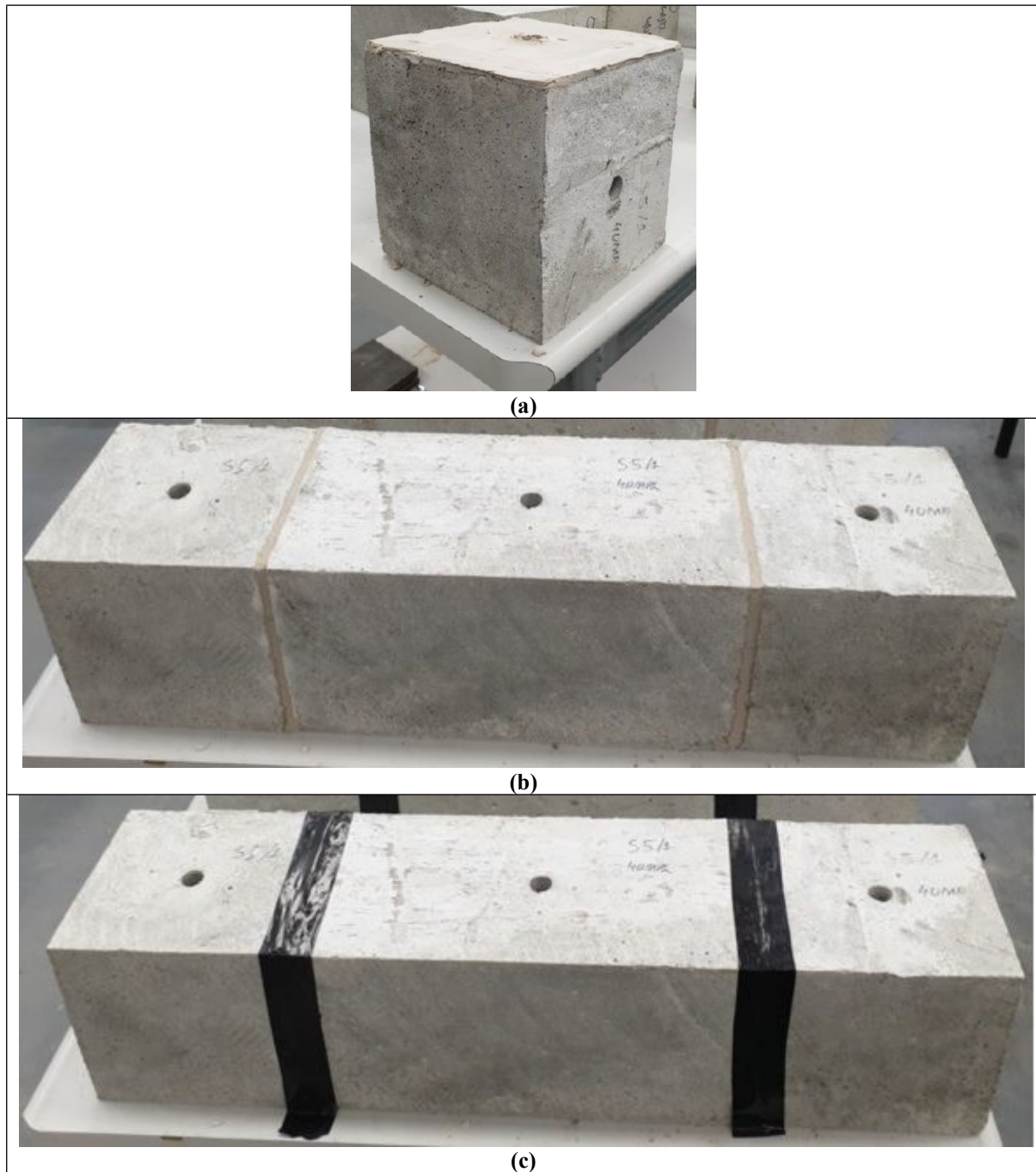


Figure 9: (a) Layer of infill material on shearing plane of concrete section;(b) Close up of the mating of the shearing planes with infill material;(c) Minimising infilled drying during preparation



Figure 10: Initial unconfined test 30-tonne



Figure 11: High quality encapsulation (left) around fibre glass bolt (right) around the concrete medium

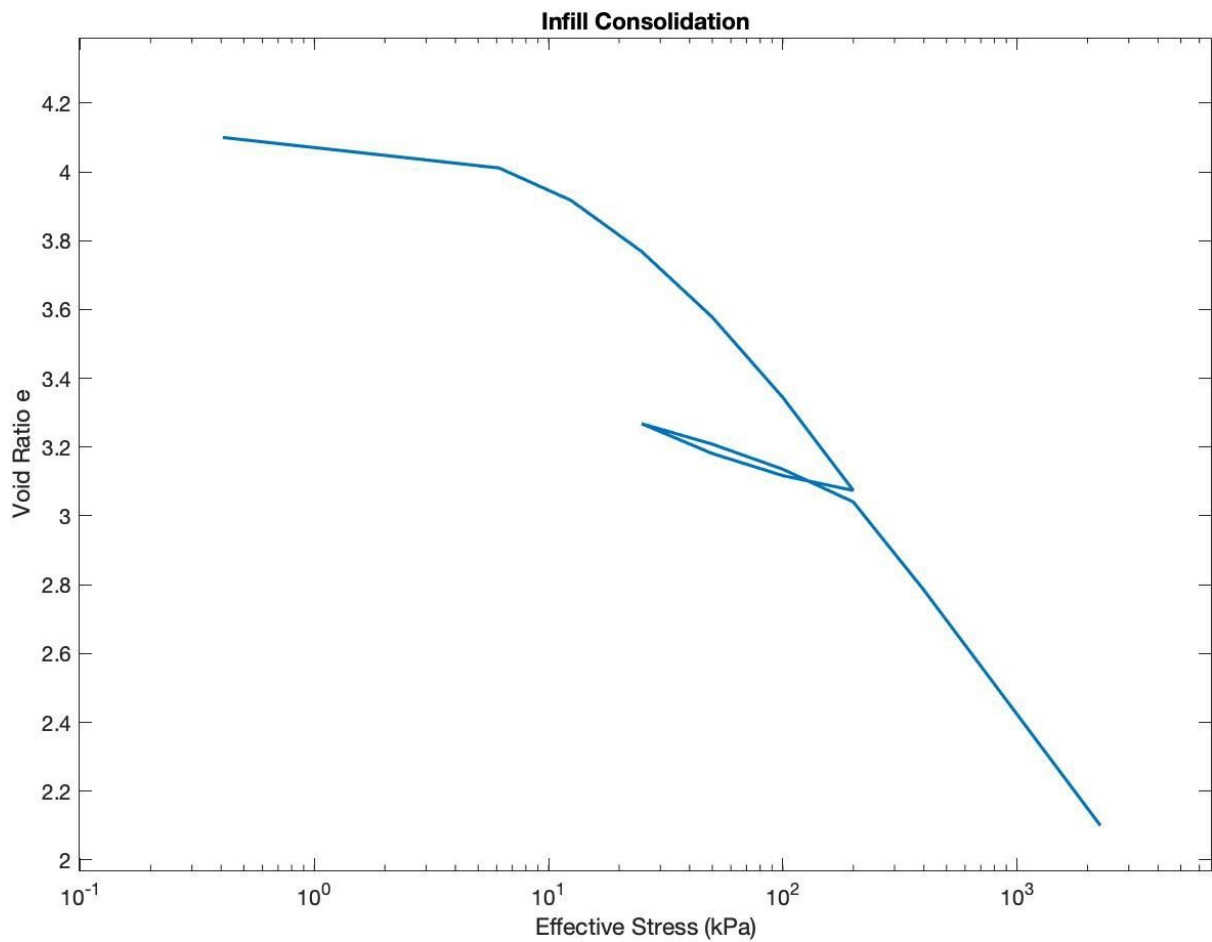


Figure 12: Consolidation test of the sandy clay infilled material

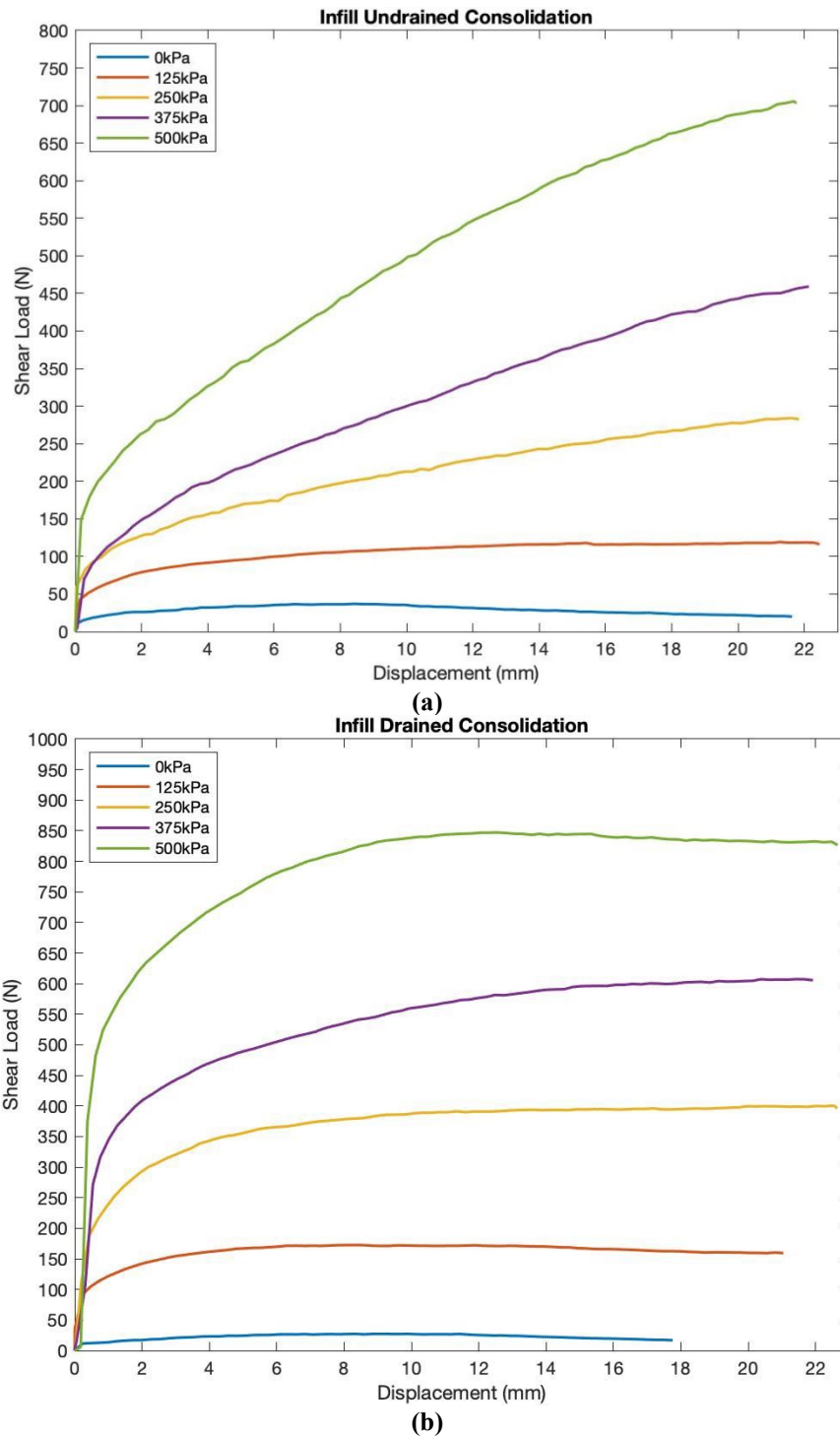


Figure 13: (a) Undrained direct shear test of infilled material; (b) Drained direct shear test of infilled material.



Figure 14: (Top) Illustration of fibreglass bolt geometry; (Bottom) Double shear testing apparatus with double ended threads

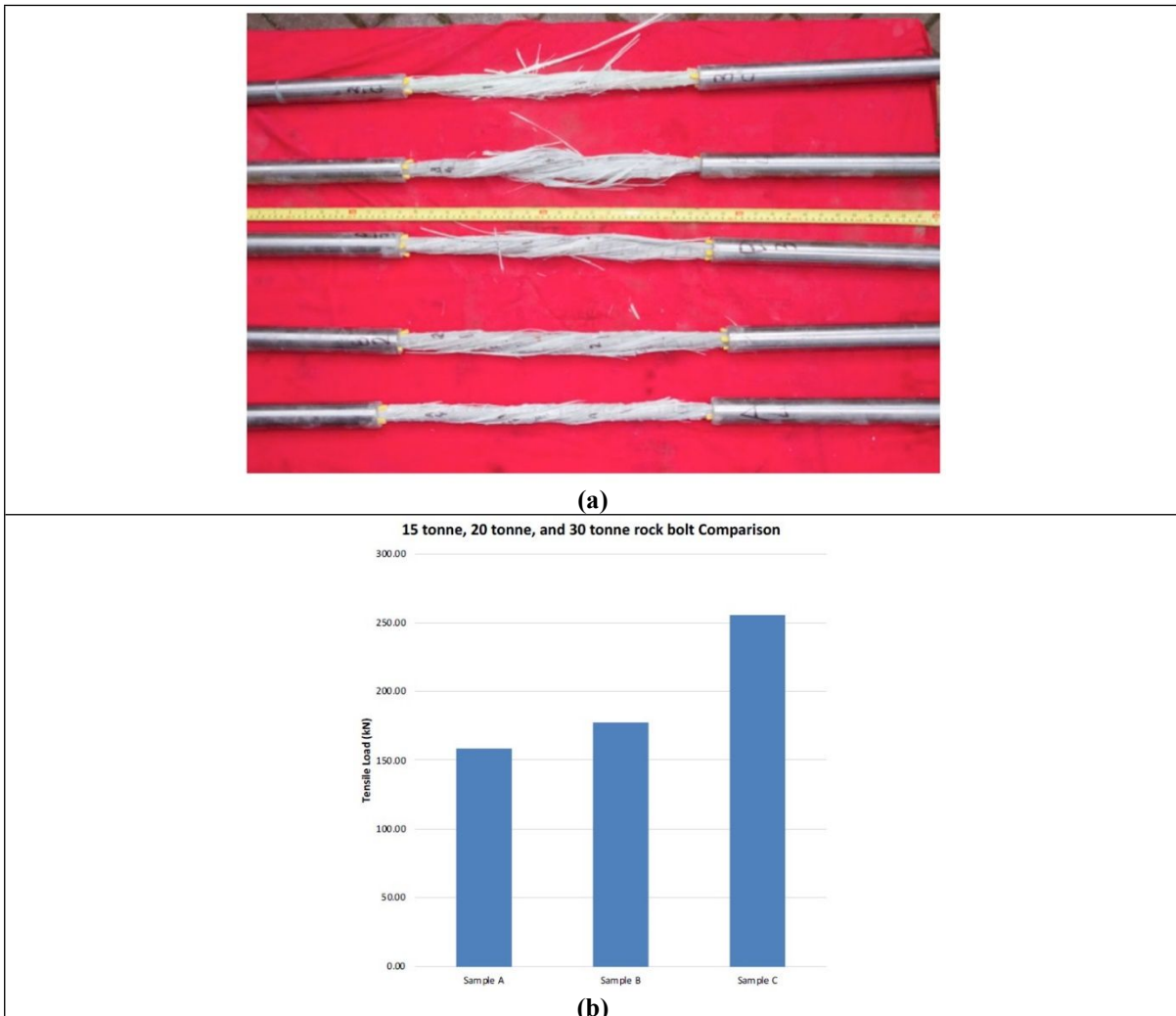


Figure 15: (a) Tensile test post failure; (b) Tensile test comparison of 15-tonne, 20-tonne, and 30-tonne rock bolts.

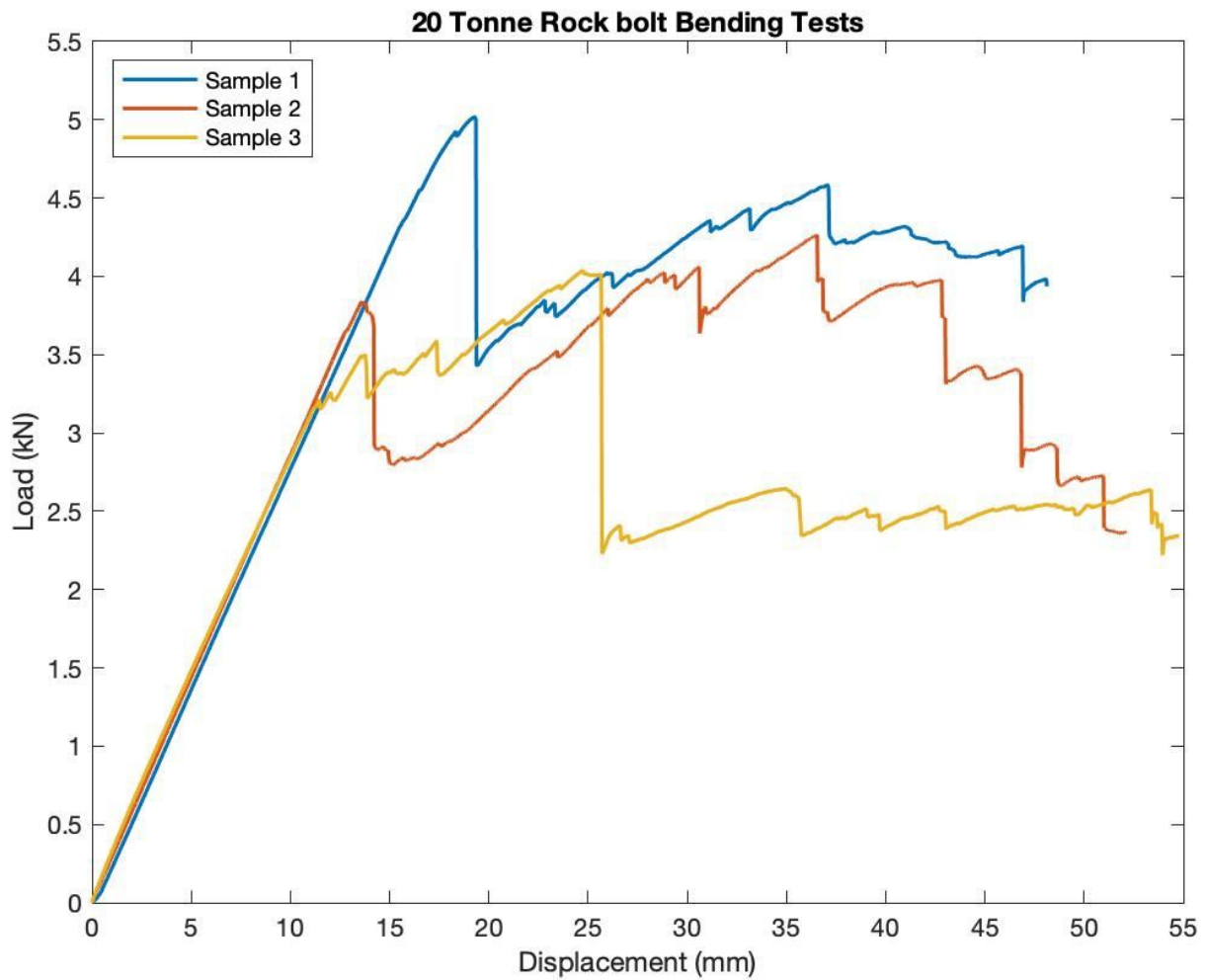


Figure 16: Rock bolt four-point bending test results.



(a)

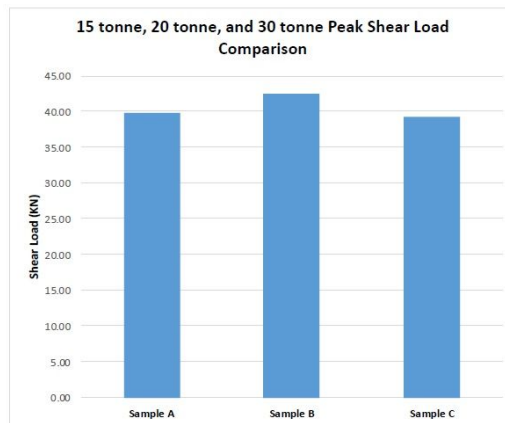


(b)

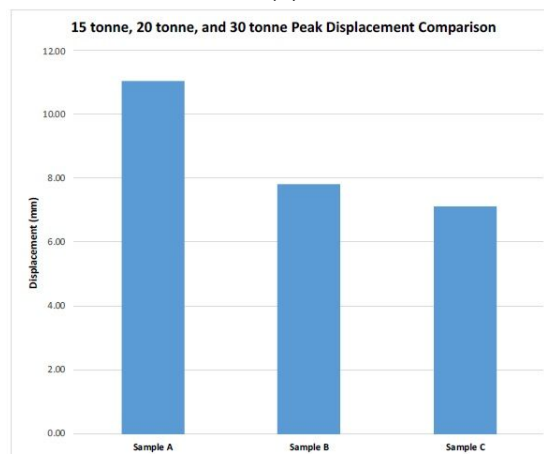
Figure 17: (a) Punch test parallel fibre sample; (b) Punch test perpendicular fibre samples.



(a)



(b)



(c)

Figure 18: (a) Single shear fibreglass samples (b) Single shear average peak load for 15-tonne, 20-tonne, and 30-tonne samples; (c) Single shear average peak displacements for 15-tonne, 20-tonne, and 30-tonne rock bolts.

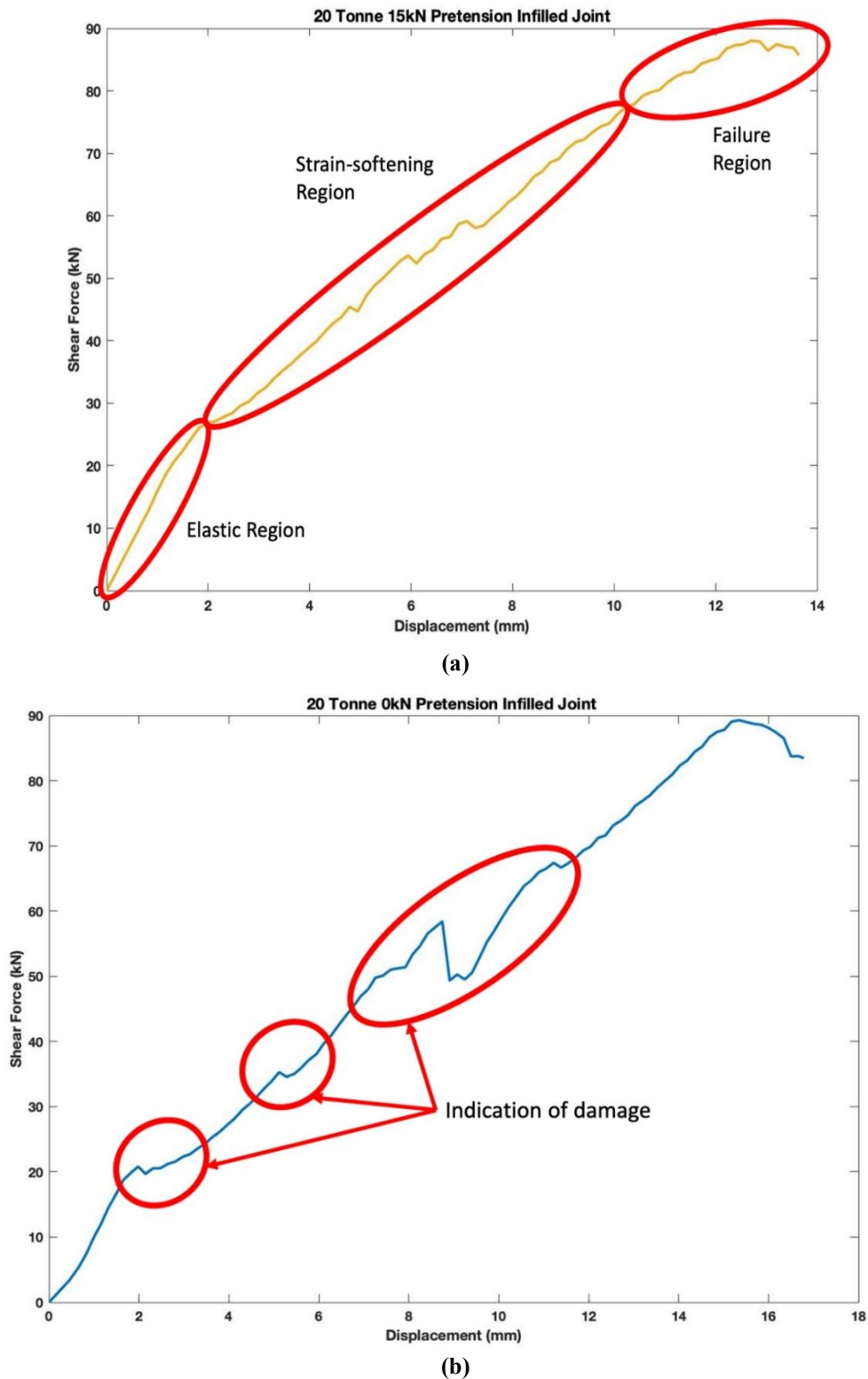


Figure 19:(a) Example of the three failure regions for 20-tonne rock bolts with infilled shear interfaces; (b) Indication of damage to sample during strain-softening stage for the 20-tonne double shear infilled sample.

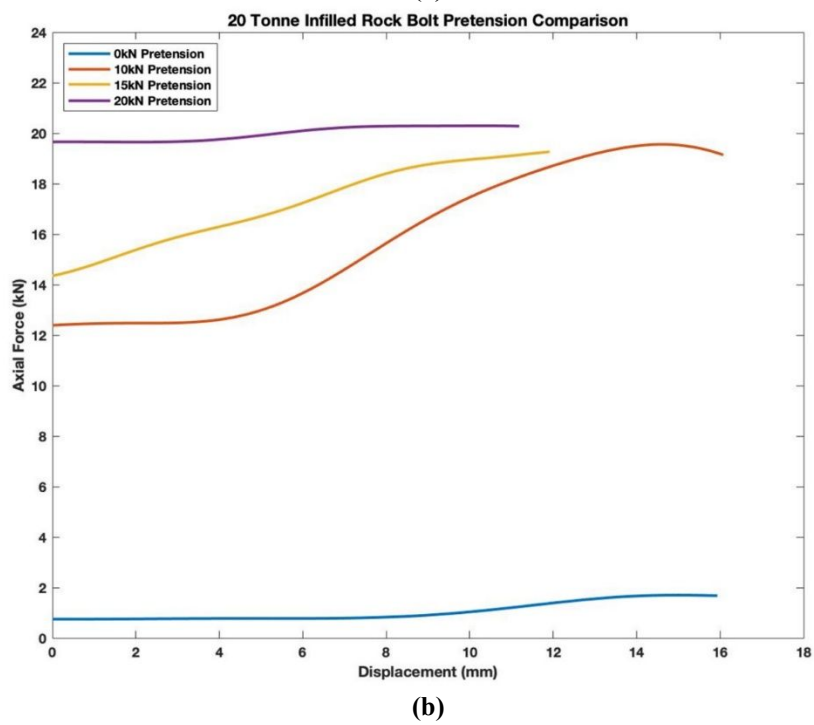
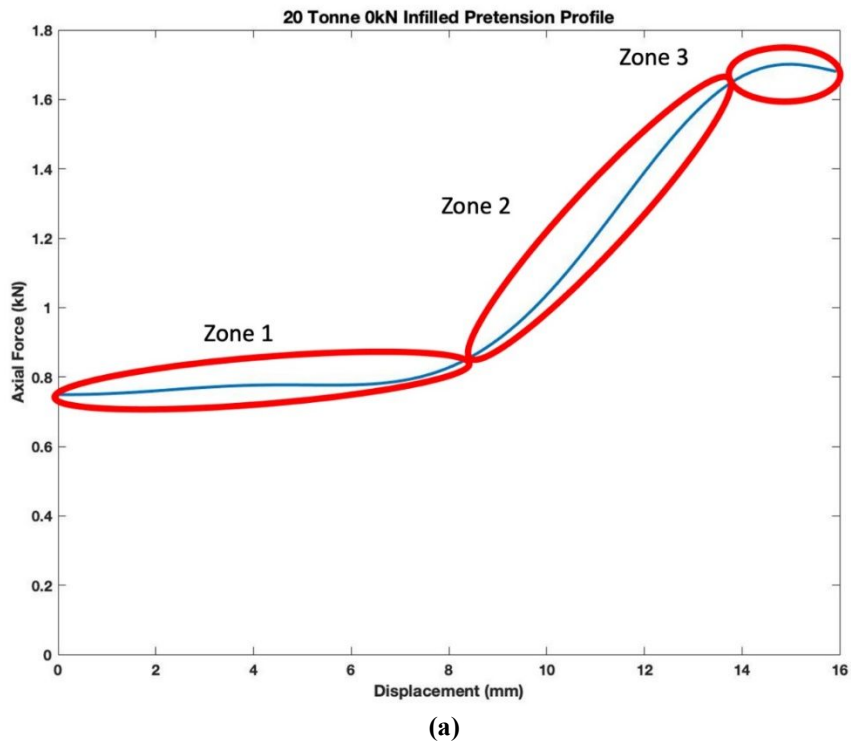


Figure 20: (a) Example of pretension zones in axial force for 20-tonne rock bolt with 0kN pretension; (b) Comparison of 20-tonne infilled pretension axial force results.

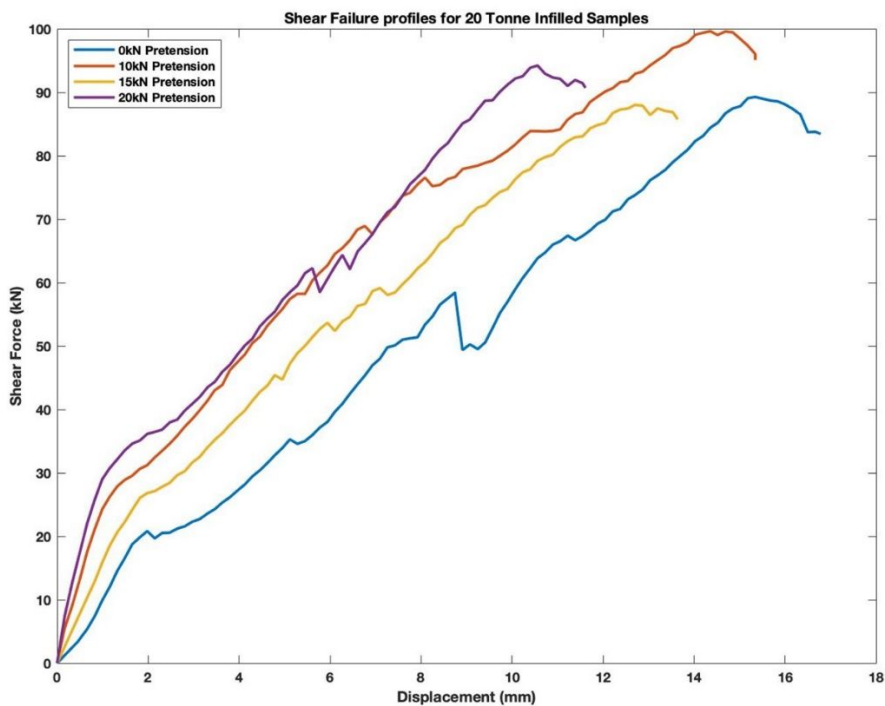


Figure 21: Shear force and displacement comparison of all 20-tonne infilled samples.

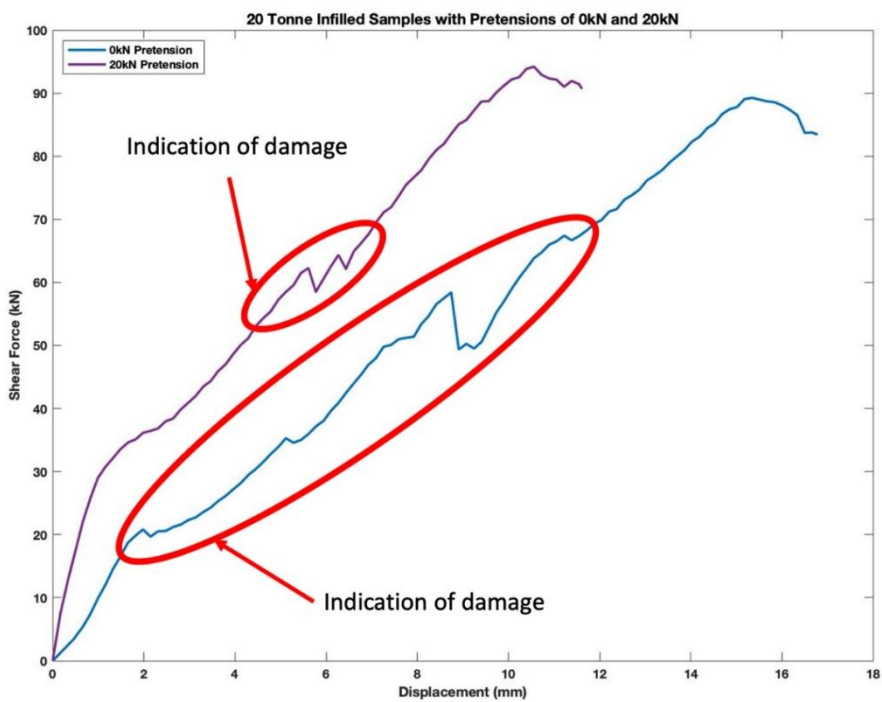


Figure 22: Change in recorded shear dip due to pretension increase from 0kN to 20kN for 20-tonne infilled rock bolts.

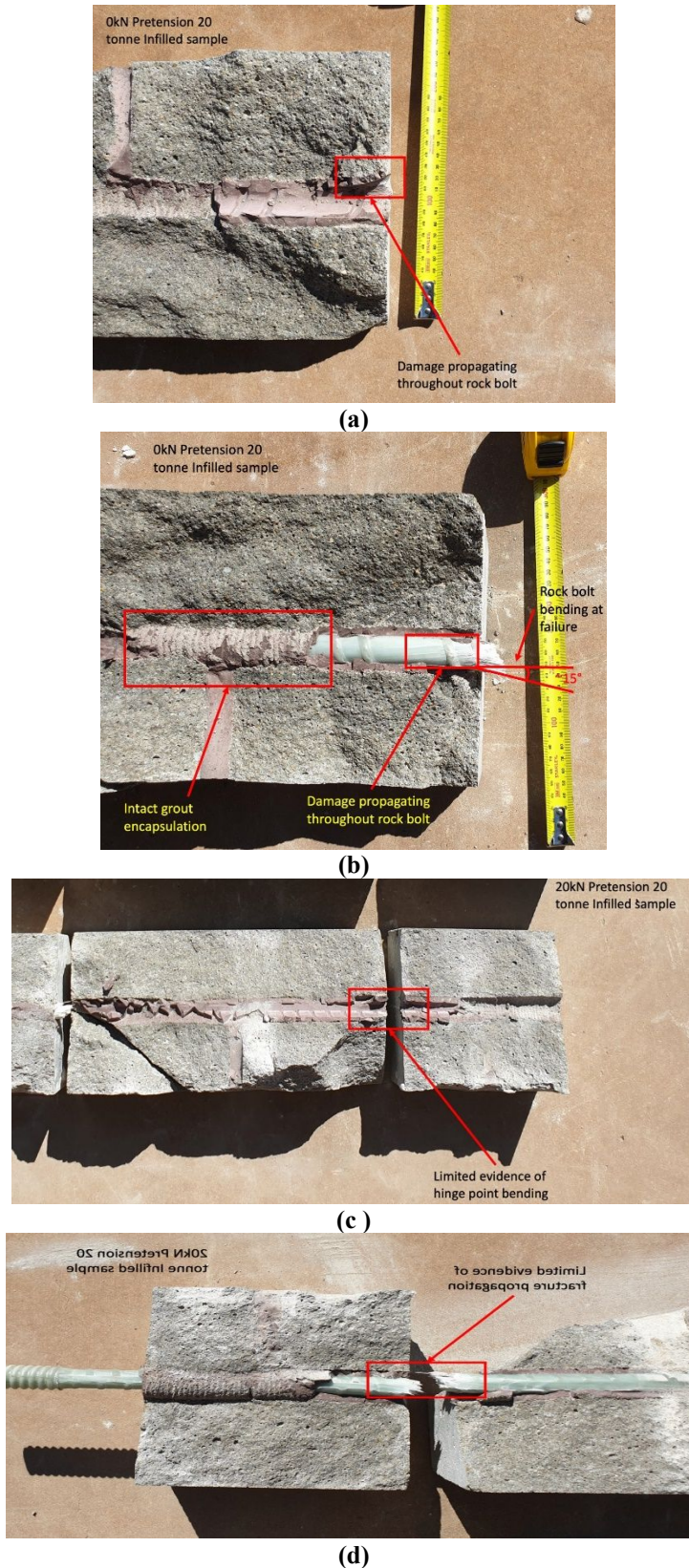
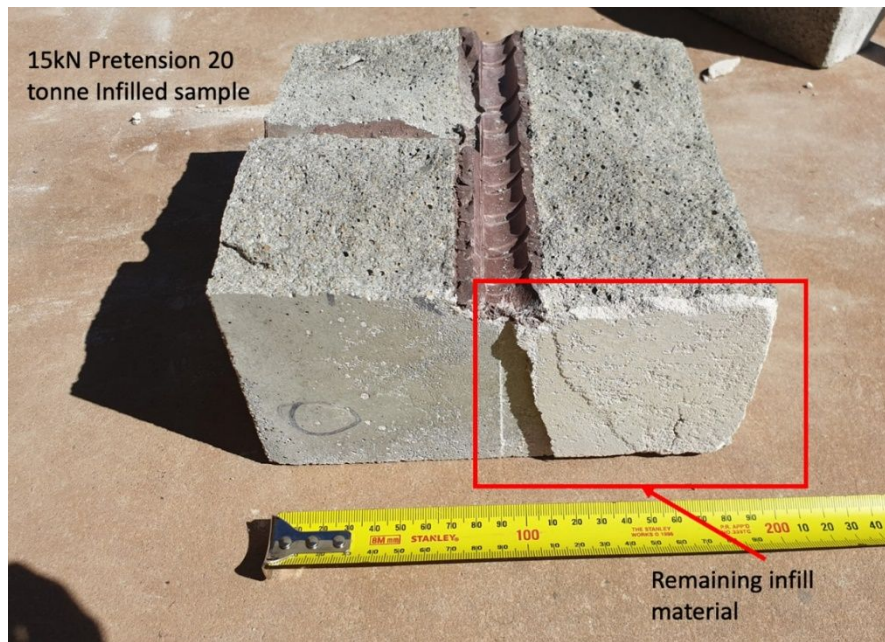
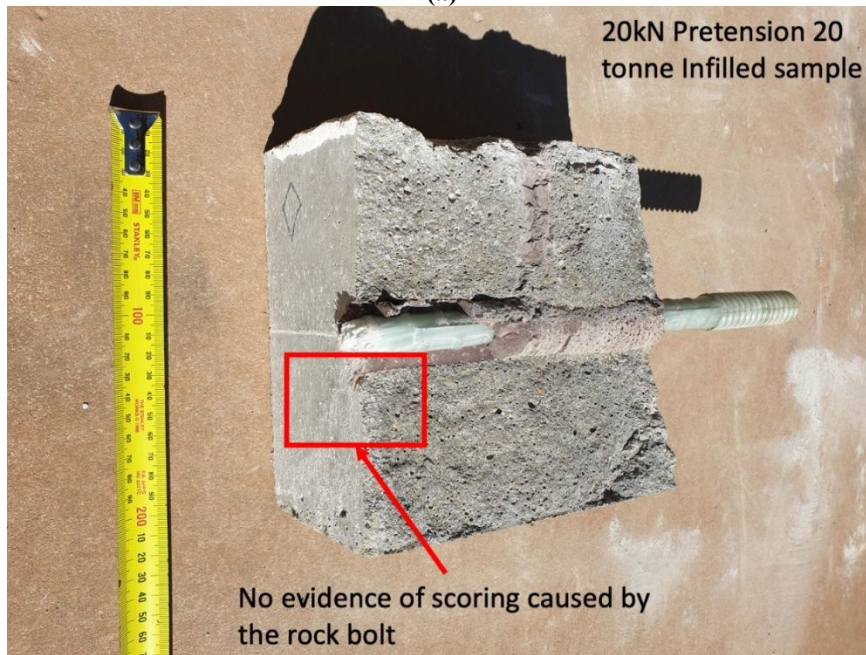


Figure 23: (a) Angle of failure and damage to grout and host rock for 20-tonne 0kN pretension infilled rock bolt sample; (b) Angle of failure and rock bolt damage for 20-tonne 0kN pretension infilled rock bolt sample; (c) Limited evidence of rotation at the hinge point for the infilled 20-tonne 20kN pretension sample; (d) Infilled 20-tonne 20kN sample demonstrating limited fracture propagation along the rock bolt element.



(a)



(b)

Figure 24: (a) Infill material that remained after disassembly of the 15kN pretension infilled 20-tonne sample; (b) No evidence of scoring caused by dragging of the fractured rock bolt end on the 20-tonne 20kN infilled sample

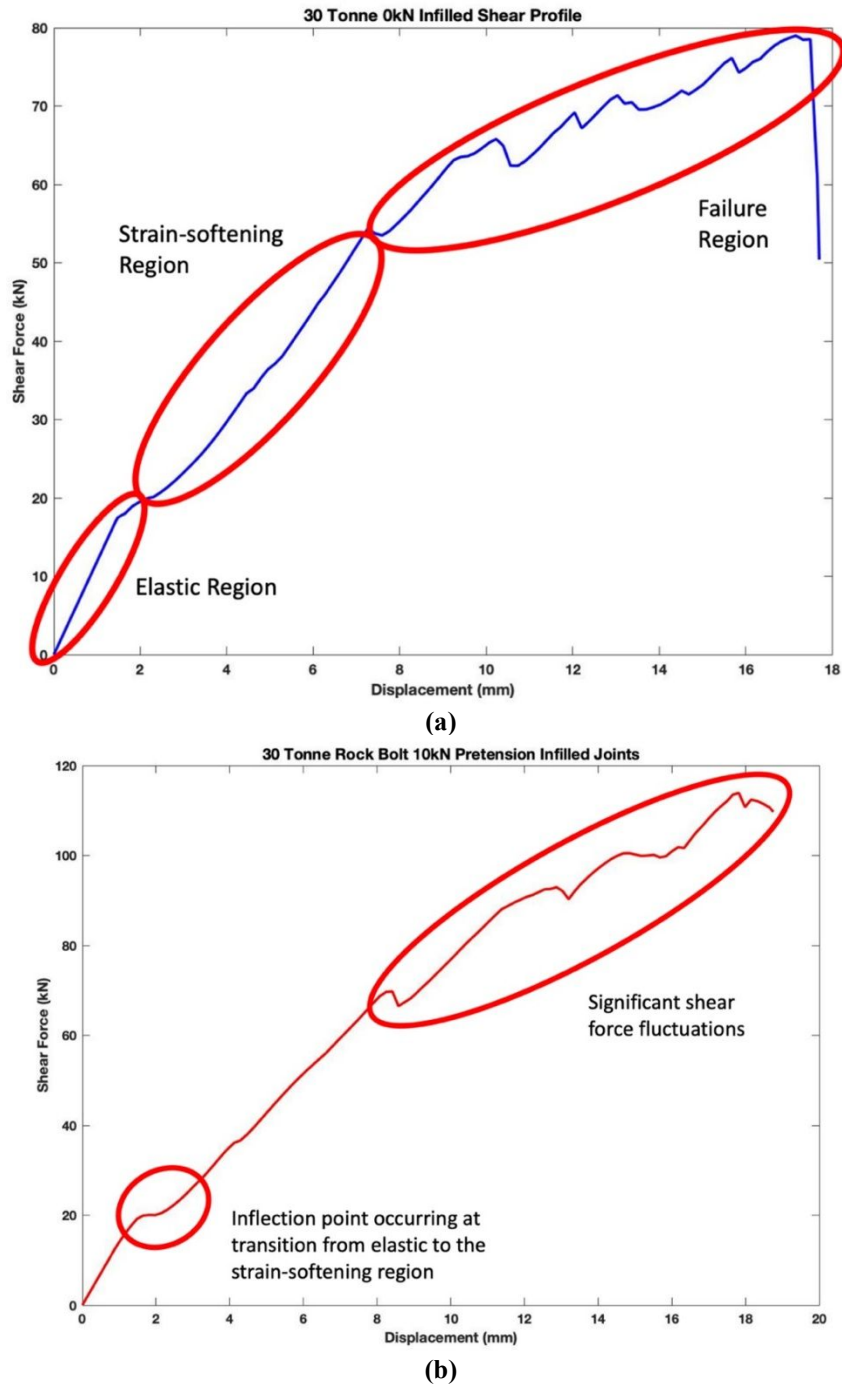
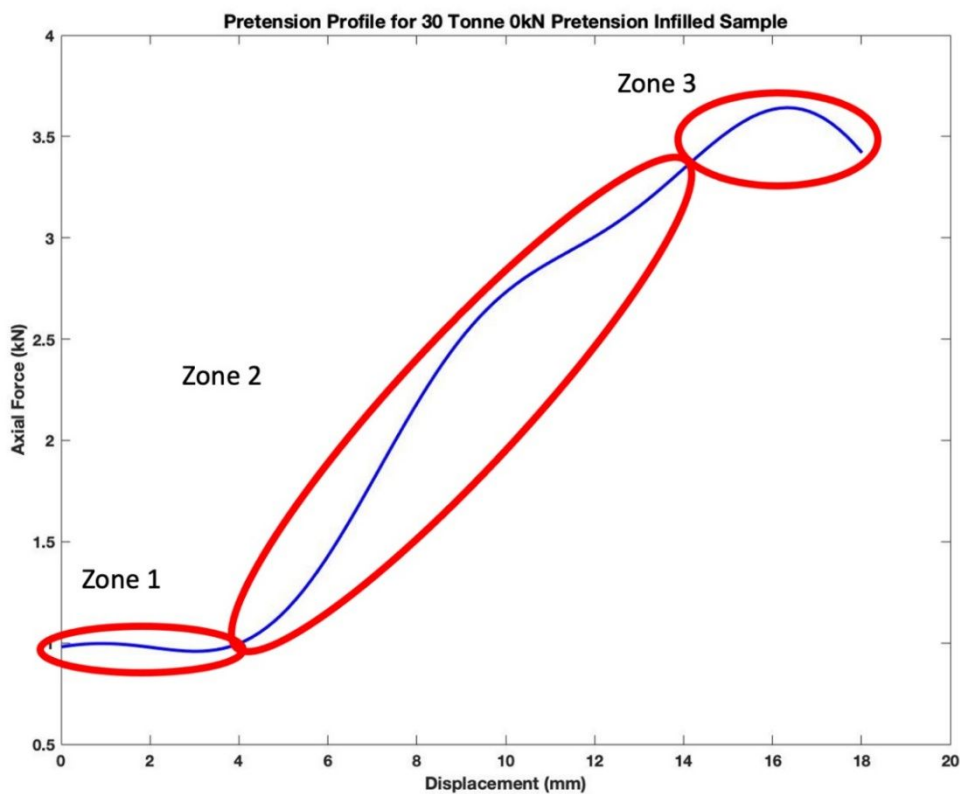
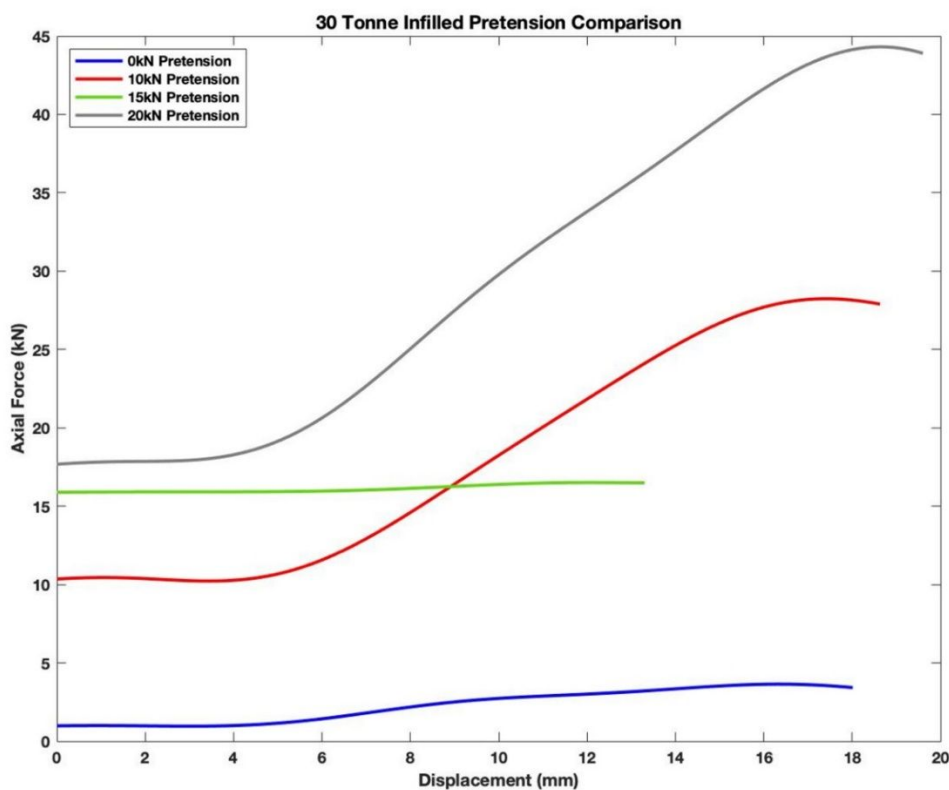


Figure 25: (a) Example of the failure regions for the 30-tonne infilled rock bolt with a pretension of 0kN; (b) Example of the inflection and fluctuations in shear force for the 30-tonne sample with 10kN pretension.



(a)



(b)

Figure 26: (a) Illustration of the pretension profile zones for the 30-tonne 0kN pretension infilled sample;(b)30-tonne rock bolt infilled pretension profile comparison.

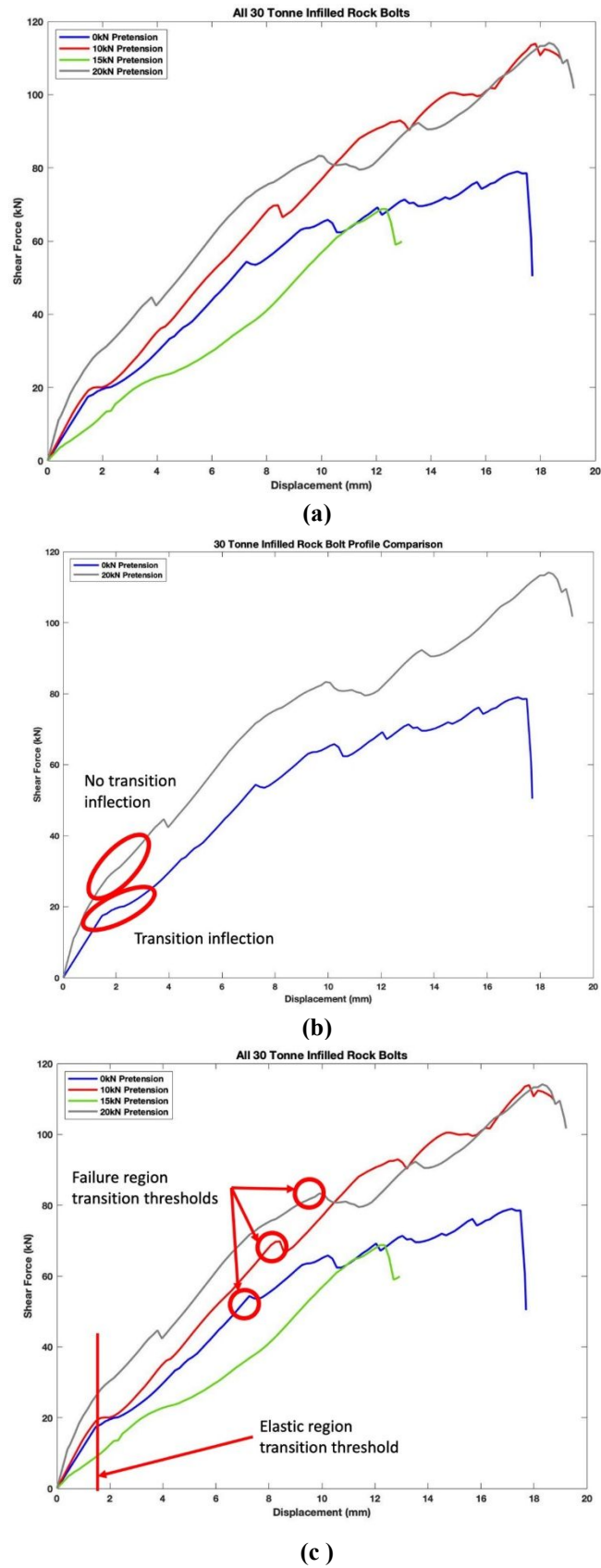
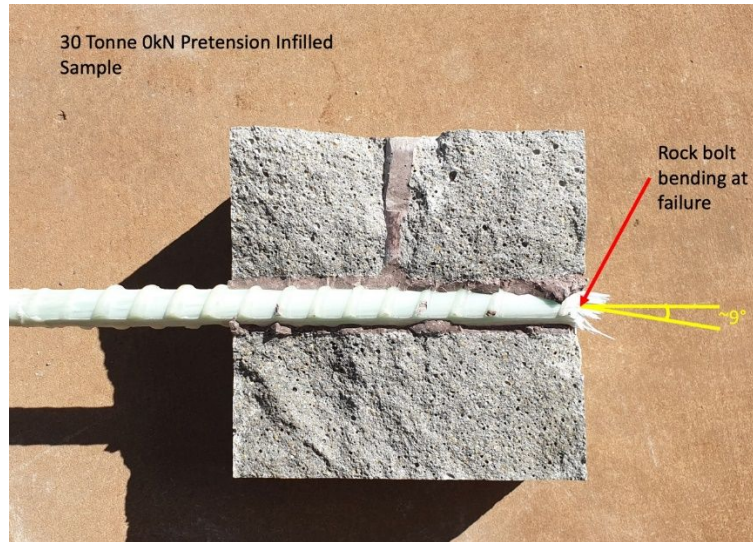
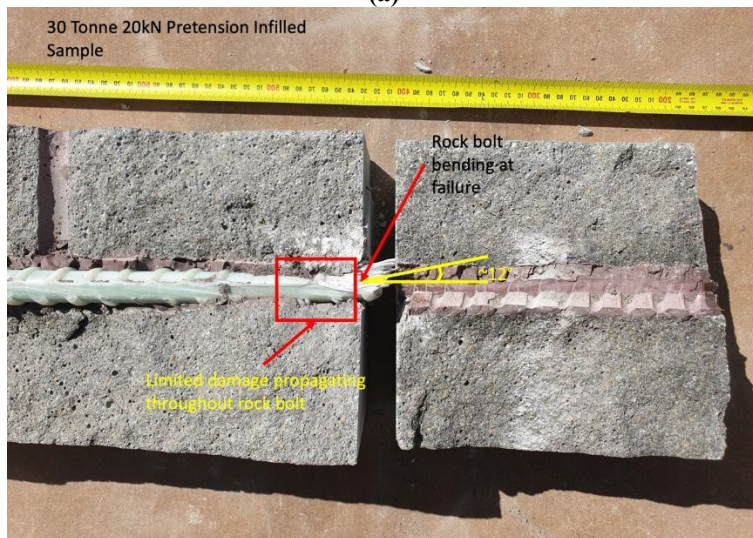


Figure 27: (a) Impact of pretension on the overall shear performance of 30-tonne rock bolts with infilled shear interfaces; (b) Impact of pretension on the elastic to strain-softening region for 30-tonne rock bolts tested with infilled shear joints; (c) The effect of pretension on the elastic region transitions for the 30-tonne rock bolts with infilled joints.



(a)

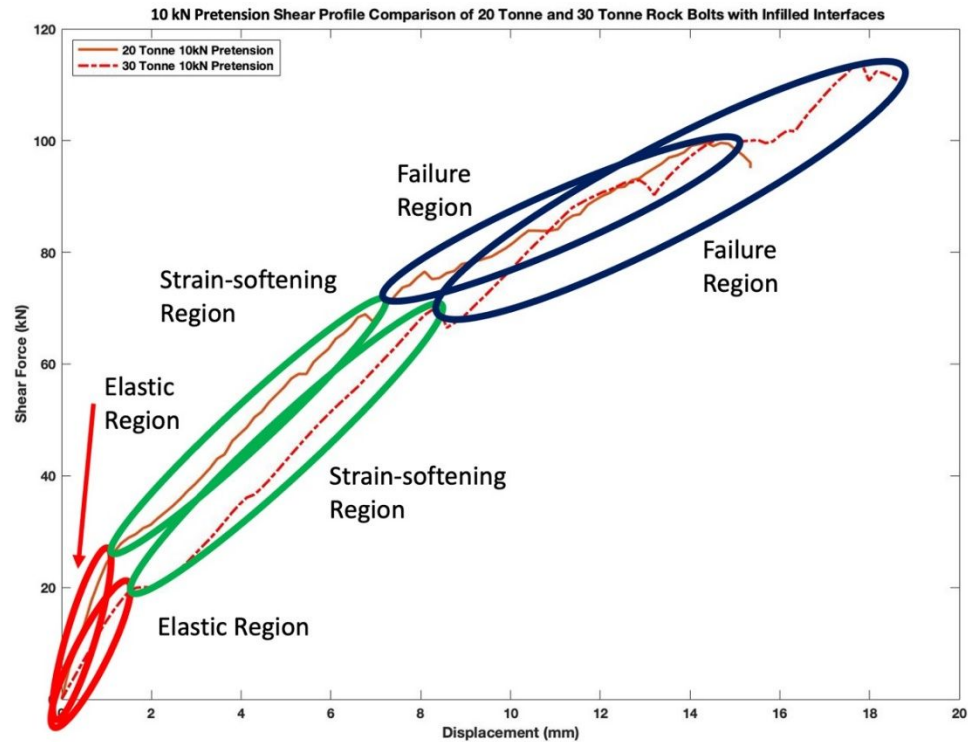


(b)

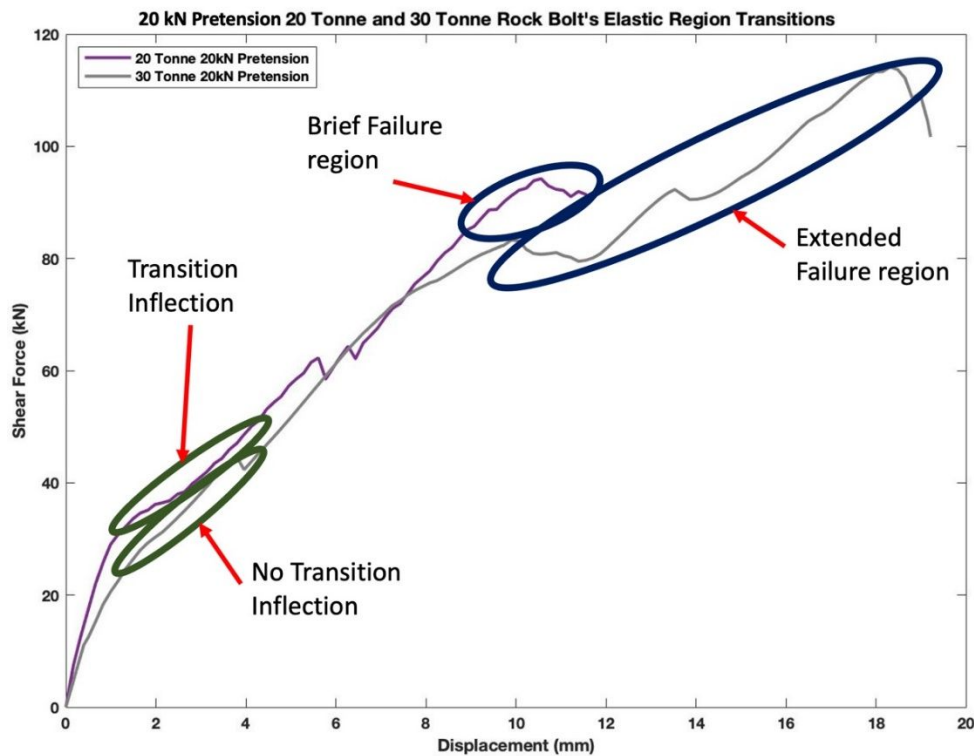


(c)

Figure 28: (a) Angle of failure for 30-tonne rock bolt with 0kN pretension with infilled shear conditions; (b) Angle of failure and damage propagation for 30-tonne rock bolt with 20kN pretension with infilled shear conditions; (c) Damage propagating through element for 30-tonne rock bolt with 0kN pretension with infilled shear conditions.



(a)



(b)

Figure 29: (a) Shear profile comparison of 10kN pretension 20-tonne and 30-tonne rock bolts with infilled Interfaces; (b) Comparison of the elastic region transition and the failure region of the 20kN pretension 20-tonne and 30-tonne rock bolts with infilled shear planes

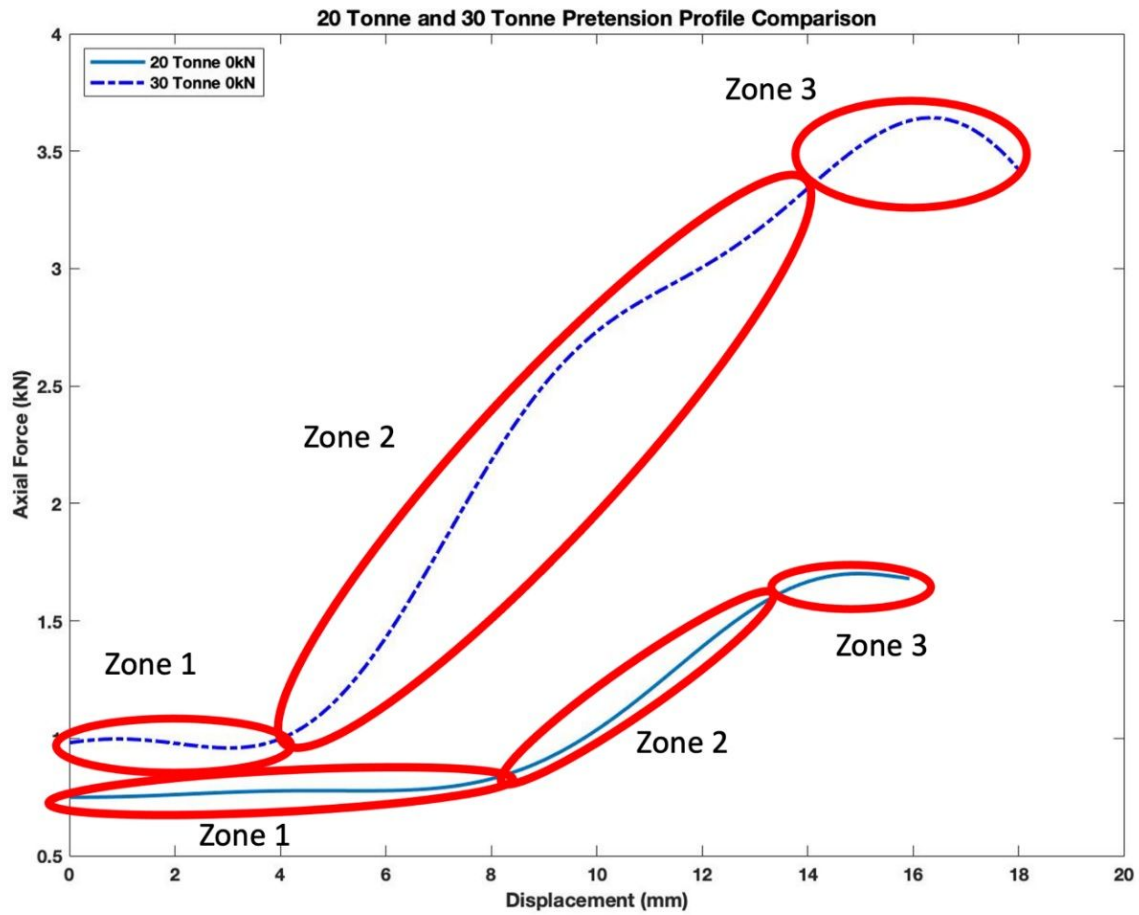


Figure 30: Comparison of the axial force profile for both 20-tonne and 30-tonne 0kN pretension samples with infilled shear planes

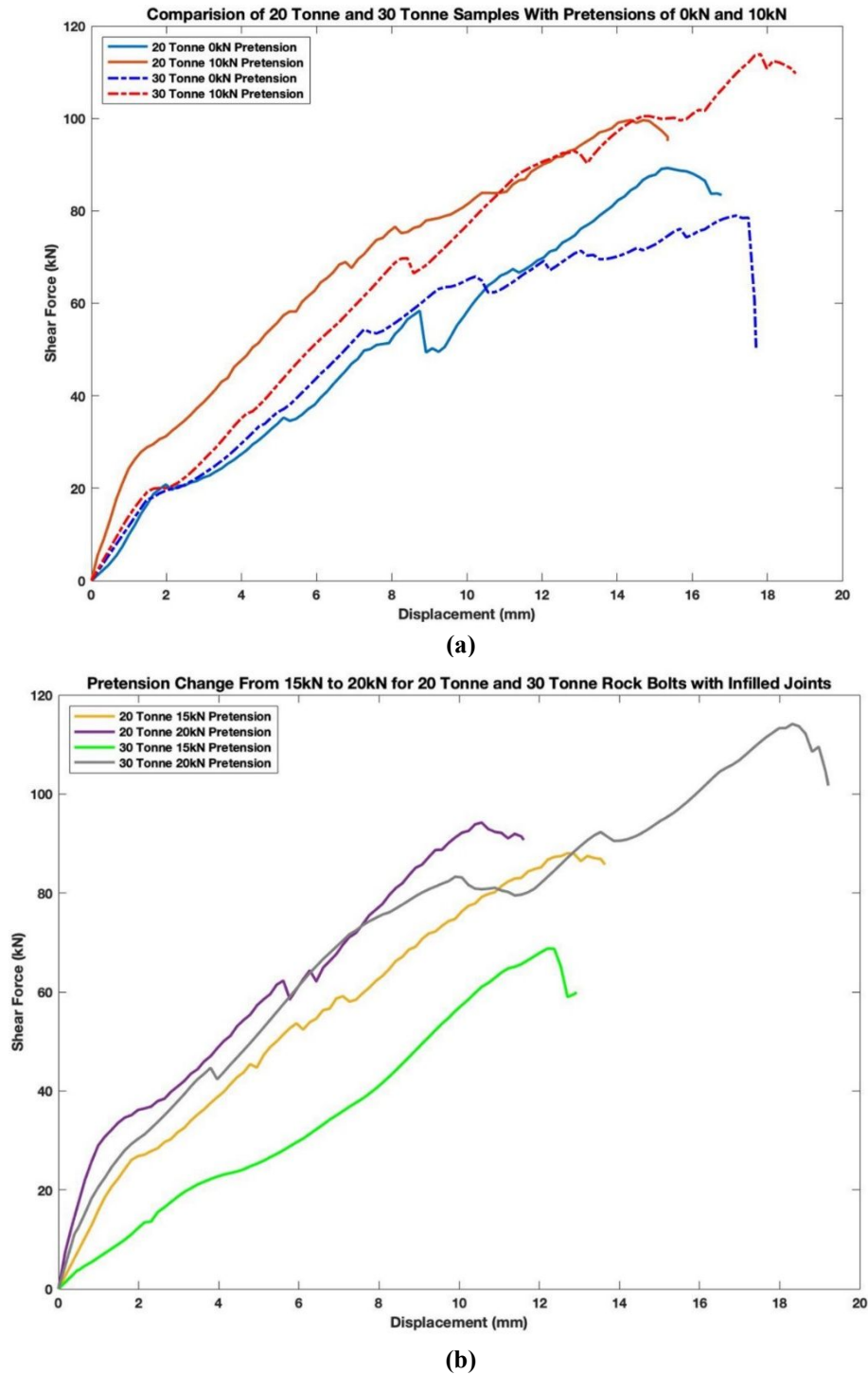
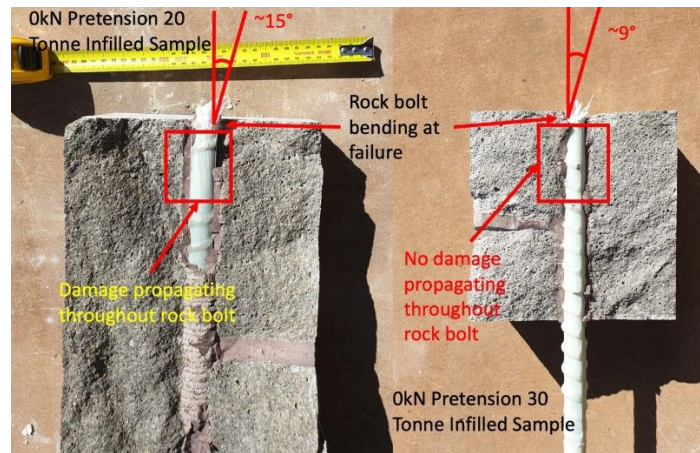


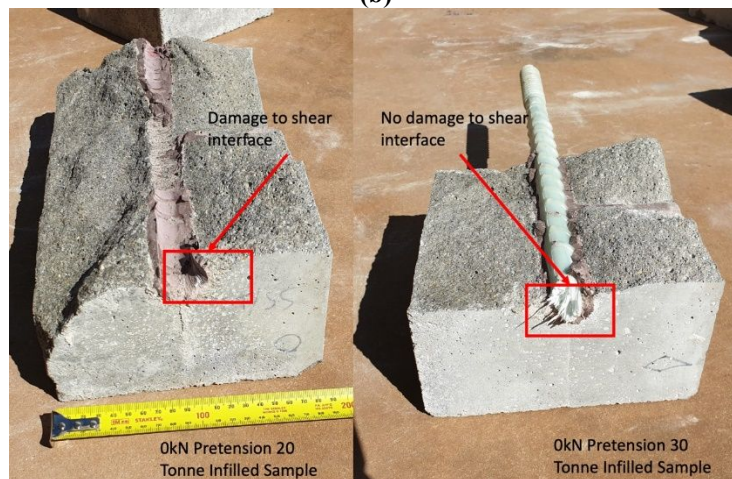
Figure 31: (a) Influence of pretension increase from 0kN to 10kN on shear force for 20-tonne and 30-tonne rock bolts with infill joints; (b) Influence of pretension increase from 15kN to 20kN on shear force for 20-tonne and 30-tonne rock bolts with infill joints.



(a)

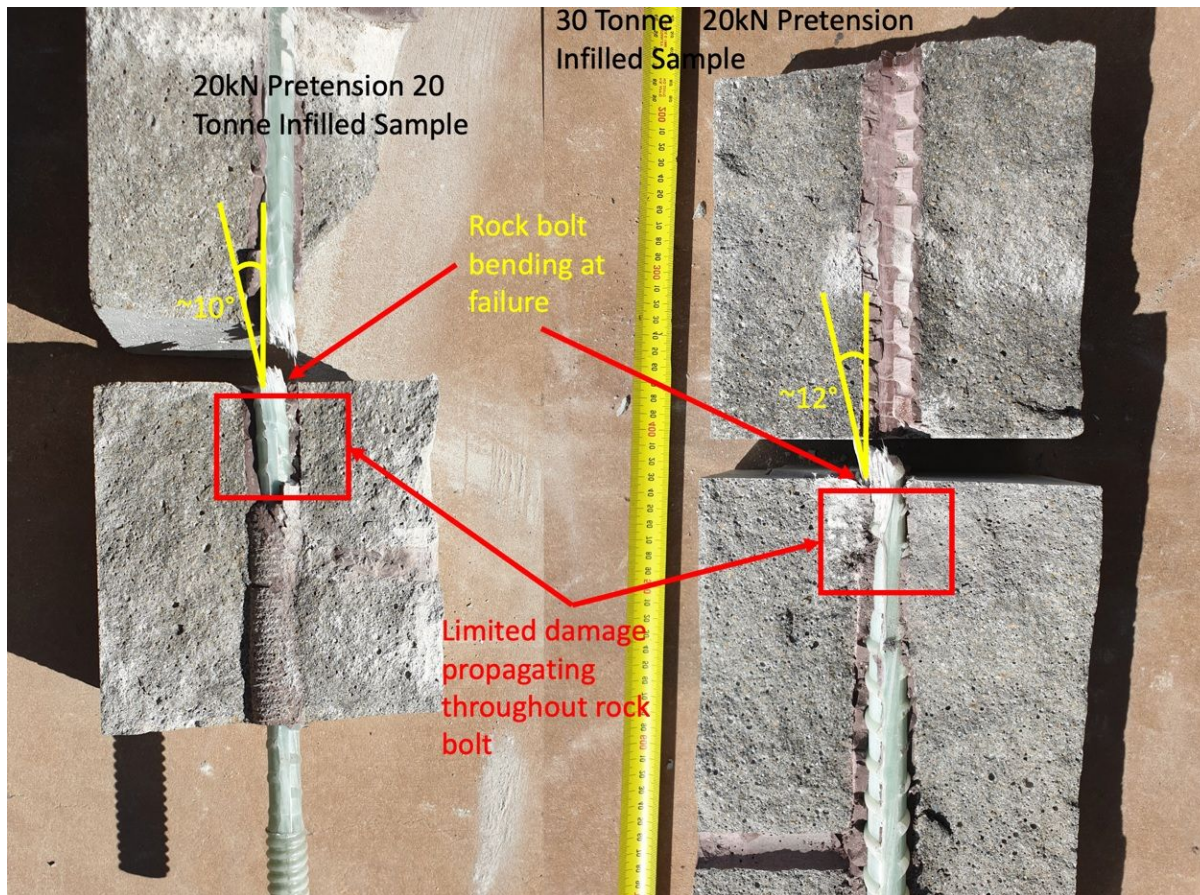


(b)

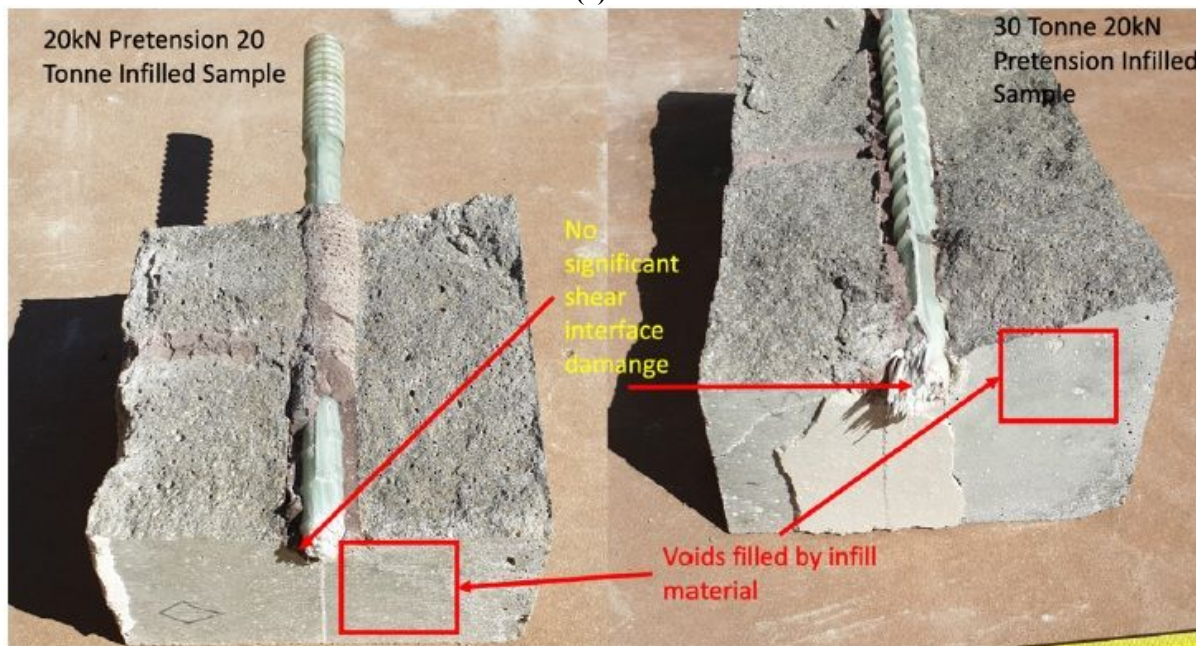


(c)

Figure 32: (a) Comparing rock bolt structural damage for 20-tonne and 30-tonne rock bolts with 0kN pretension and infilled shear interfaces; (b) Representation of rock bolt damage for 30-tonne rock bolt with infilled shear interfaces and 0kN pretension; (c) Comparing shear plane damage of 20-tonne and 30-tonne rock bolts with infilled shear interfaces and 0kN pretension.



(a)



(b)

Figure 33: (a) Comparing rock bolt hinge point and rock bolt damage for 20-tonne and 30-tonne rock bolts with 20kN pretension and infilled shear interfaces; (b) Comparing shear plane damage of 20-tonne and 30-tonne rock bolts with 20kN pretension and infilled shear interfaces.